Annu. Rev. Earth Planet. Sci. 1999. 27:149–82

THE DEGLACIATION OF THE NORTHERN HEMISPHERE: A Global Perspective

Richard B. Alley[1] *and Peter U. Clark*[2]
[1]Earth System Science Center and Department of Geosciences, The Pennsylvania State University, University Park, Pennsylvania 16802; e-mail: ralley@essc.psu.edu
[2]Department of Geosciences, Oregon State University, Corvallis, Oregon 97331; e-mail: clarkp@ucs.orst.edu

KEY WORDS: paleoceanography, paleoclimatology, ice ages, Heinrich events, Dansgaard-Oeschger events

ABSTRACT

Orbitally induced increase in northern summer insolation after growth of a large ice sheet triggered deglaciation and associated global warming. Ice-albedo, sea-level, and greenhouse-gas feedbacks, together with tropical warming from weakening winds in response to polar amplification of warming, caused regional-to-global (near-) synchronization of deglaciation. Effects were larger at orbital rather than millennial frequencies because ice sheets and carbon dioxide vary slowly. Ice-sheet–linked changes in freshwater delivery to the North Atlantic, and possibly free oscillations in the climate system, forced millennial climate oscillations associated with changes in North Atlantic deep water (NADW) flow. The North Atlantic typically operates in one of three modes: modern, glacial, and Heinrich. Deglaciation occurred from a glacial-mode ocean that, in comparison to modern, had shallower depth of penetration of NADW formed further south, causing strong northern cooling and the widespread cold, dry, and windy conditions associated with the glacial maximum and the cold phases of the millennial Dansgaard-Oeschger oscillations. The glacial mode was punctuated by meltwater-forced Heinrich conditions that caused only small additional cooling at high northern latitudes, but greatly reduced the formation of NADW and triggered an oceanic "seesaw" that warmed some high-latitude southern regions centered in the South Atlantic.

0084-6597/99/0515-0149$08.00

Introduction

Complex processes and feedbacks in the coupled Earth system involving atmosphere, ocean, ice, land surface, and biota caused northern-hemisphere and global deglaciation. Long-term geological changes produced conditions favorable for the recent ice ages. Over the last million years, warming and cooling have occurred with strong periodicities ranging from about 1500 years to about 100,000 years. The slower variations appear to have been driven by changes in the distribution of sunlight on Earth associated with features of the Earth's orbit (Hays et al 1976, Lorius et al 1990, Imbrie et al 1992, 1993). The faster variations are plausibly related to changes in ice sheets and in the deep circulation of the ocean. The deglaciation must be understood as a superposition of these and other variations.

We briefly summarize the orbital hypothesis and its implications for nearly synchronous global climate change. We then review the characteristics and possible mechanisms of the faster variations in terrestrial and marine environments. Changes in freshwater fluxes to the oceans during the last deglaciation provided links between these environments. The hemispheric phasing of responses to this forcing provides further clues to the mechanisms involved, but raises additional questions about near-synchrony at orbital frequencies. Identification of atmospheric and shallow-ocean mechanisms synchronizing the hemispheres leads to an overview of deglaciation.

Milankovitch Control

Most relevant research shows that features of Earth's orbit cause changes in the seasonality of incoming solar radiation that control glacial cycles (the Milankovitch or Milankovitch-Croll model). Some of the forcing is out of phase between the hemispheres. Climate has cooled and ice has grown globally when middle and high northern latitudes had short, cool summers, with global warming and ice shrinkage linked to long, hot northern summers (Imbrie et al 1992, 1993). A complicating factor—that large seasonality variations with periodicity of 19,000, 23,000, and 41,000 years caused small climate changes, but small variations with 100,000-year periodicity caused large climate changes—is likely explained by the effects of the ice sheets themselves, particularly the tendency of large ice sheets that have depressed the Earth's crust and warmed their beds to change more rapidly than smaller ice sheets (reviewed by Imbrie et al 1992, 1993; also see Tarasov & Peltier 1997).

Global changes have not been entirely synchronous, and the detailed phasing provides critical information on mechanisms (Imbrie et al 1992, 1993), but the near-synchrony is striking. For example, Genthon et al (1987) and Lorius et al (1990) attempted to explain the stable isotopic record of ice from the Vostok ice core, a proxy for temperature at high southern latitude, as a linear superposition

of possible controlling variables (northern insolation, southern insolation, atmospheric carbon dioxide concentration, etc.) with weighting determined by multiple regression. Uncertainties were introduced by difficulties in dating and choice of members for the set of possible controlling variables. Nonetheless, through a range of models it proved necessary to include a northern control as well as a southern one to explain southern temperature. Most of the variance of the Vostok isotopic record is well explained by changes in greenhouse-gas concentrations and global ice volume, which in turn are largely linked to northern insolation and ice-sheet processes. Strong covariation of CO_2 and ice volume prevented clear identification of their relative importance.

Global cooling and warming have been caused by little net change of incoming solar radiation, so large positive feedback must have been active. Sea-level changes, ice-albedo feedbacks, and changes in greenhouse gases likely were important. Below we discuss these and other mechanisms, and how they may have contributed to the global near-synchrony of climate changes at orbital frequencies. However, explaining southern temperatures requires consideration of southern as well as northern influences (Genthon et al 1987).

Most available data support this broad picture, with a possible exception: At one site in Nevada, groundwater isotopes shifted to heavier values before summertime insolation began rising at the end of the previous glaciation (Winograd et al 1992). This exception may reflect non-temperature effects in the records (Grootes 1993) or other complications. The orbital features also might have caused variations in the extraterrestrial dust encountered by Earth (Muller & McDonald 1997), but available sedimentary evidence does not show large changes in dust accretion (Marcantonio et al 1996). The Milankovitch model remains the best description of the ice-age cycles over tens to hundreds of millennia. A deglaciation—a major, rapid reduction in ice volume—has occurred each time northern-summer insolation rose significantly after a big ice sheet had grown (Raymo 1997). However, the picture is less clear for more rapid climate changes, which we review next.

Heinrich-Bond and Dansgaard-Oeschger Cycles

Deglaciation has not been monotonic. Early European work documented returns to cold conditions, such as the Younger Dryas (YD) interval. Longer records show that such millennial variability has been quite common, especially during orbitally driven coolings and warmings (Figure 1). Prominent events have had an approximate spacing of 1500 years (Dansgaard-Oeschger oscillations) (Bond & Lotti 1995, Bond et al 1997, Grootes & Stuiver 1997, Mayewski et al 1997), and of a few thousand years (Heinrich-Bond cycles) (Heinrich 1988, Bond et al 1993). Whether these are true periodicities phase-locked to the calendar, or whether they are simply general bands in which variability has occurred

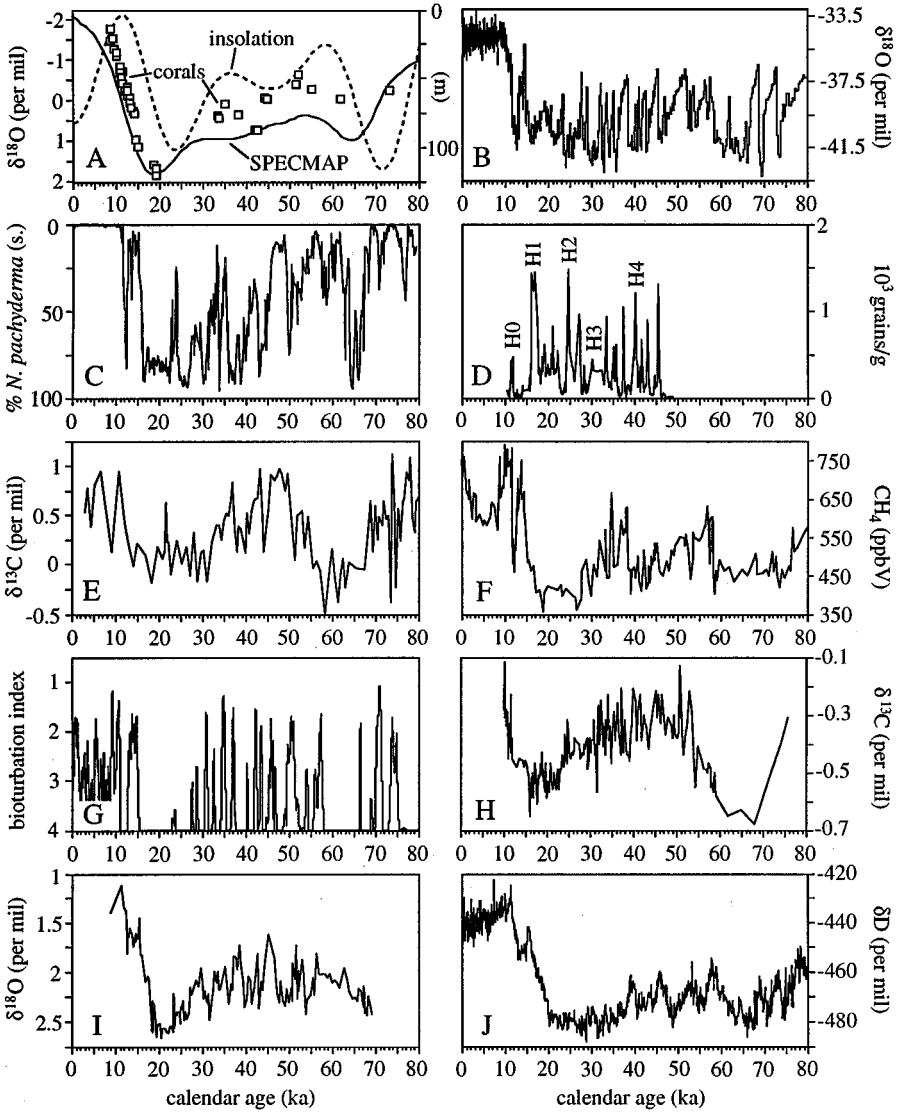

(Heinrich 1988, Mayewski et al 1997), is a question yet unanswered. Evidence on meltwater routing (discussed below) favors variability in a general band, as does observed variability in spacing (e.g. from 700 to 2200 years for the Holocene events of Bond et al 1997).

The coolings of the Dansgaard-Oeschger (D-O) cycles have been marked by abrupt terminations, and often by abrupt onsets (Figure 1*b*). For example, the termination of the YD—a prominent event that may also have been a Heinrich event (H event)—about 11.5 thousand calendar years before present (cal kyear) in central Greenland involved 5 to 10°C warming, accumulation-rate doubling, threefold (fine-grained dust and sea salt) to sevenfold (coarse-grained dust, calcium) drop in windblown materials, and other changes, with most of the change occurring in only a few years (Alley et al 1993, 1995; Mayewski et al 1997; Taylor et al 1997; Severinghaus et al 1998). Methane began a large (40 percent) rise at the end of the YD (Figure 1*f*), 0 to 30 years (<1 sample) after the warming in Greenland (Severinghaus et al 1998). Because the low-latitude hydrologic cycle was probably involved in the methane rise (Chappellaz et al 1993), one can argue for a widespread to globally significant and synchronous event.

Large changes are recorded at about the same time from widespread regions across much of the northern hemisphere and into the southern (e.g. Peteet 1993, Denton & Hendy 1994). In general, YD conditions were cold, dry, or windy compared to modern across much of the Earth. The drop in windiness

←

Figure 1 Climate records covering the last 80,000 calendar years. (*a*) Insolation (June, 60°N) (vertical scale, not shown, ranges from 450 to 515 W/m^2), SPECMAP stack of the global ice volume signal (δ^{18}O in per mil) (Imbrie et al 1984), and U/Th ages on raised corals (elevations corrected for tectonic uplift) from Barbados (Bard et al 1993) and New Guinea (Edwards et al 1993; Chappell et al 1996) showing changes in sea level. (*b*) GISP2 δ^{18}O record (Grootes et al 1993). (*c*) Changes in the percentage of *Neogloboquadrina pachyderma* (s.) from North Atlantic core VM23-081 (Bond et al 1993). (*d*) Concentrations of lithic grains (in numbers of grains >150 μm per gram of sediment) from North Atlantic core VM23-081. Data from Bond & Lotti (1995). Radiocarbon ages calibrated to calendar ages using relation of Bard et al (1997). Given uncertainties in calibrating radiocarbon ages on marine shell material to calendar years, we do not expect a perfect correlation of timescales. However, recent additional radiocarbon calibration in the interval from 10 to 30 cal kyear (Kitagawa & van der Plicht 1998) strongly supports the calibration from paired U-Th and ^{14}C ages on corals (Bard et al 1993). (*e*) δ^{13}C data for *Cibicidoides wuellerstorfi* from equatorial Atlantic core EW9209-1JPC (5°N) (Curry & Oppo 1997). (*f*) GISP2 record of variations in atmospheric methane (Brook et al 1996). (*g*) Changes in bioturbation index from ODP Site 893 (Santa Barbara basin) (1 = laminated sediments, 4 = massive sediments) (Behl & Kennett 1996). (*h*) δ^{13}C record (*Cibicidoides wuellerstorfi*) from northeastern Pacific core W8709A-13PC (Lund & Mix 1998). (*i*) δ^{18}O data for *Neogloboquadrina pachyderma* from Southern Ocean core RC11-83 (~42°S) (Charles et al 1996). (*j*) Vostok, Antarctica, δD record (data from Jouzel et al 1987, age model from Bender et al 1994).

documented in the Cariaco Basin off Venezuela, at the same time within the dating uncertainties of about a century, occurred in less than a decade (Hughen et al 1996).

Growing evidence indicates that this YD pattern occurred for most or all of the D-O events (e.g. Chappellaz et al 1993). The geographic pattern of the cold event about 8.2 cal kyear is quite similar to that of the YD (e.g. Alley et al 1997). Over the available record, virtually all of the D-O coolings are recorded in sediments from the Santa Barbara Basin, off the coast of California (Figure 1*g*), as times of enhanced bioturbation related to enhanced oxygenation of these shallow waters (475 m modern sill depth; Behl & Kennett 1996). The cold phases of the D-O oscillations in the North Atlantic were marked by increased iceberg rafting of debris into a cold, fresh surface ocean (Figures 1*c*, 1*d*), and by reduced formation of North Atlantic deep water (NADW) (e.g. Lehman & Keigwin 1992b, Oppo & Lehman 1995, Bond et al 1993, Bond & Lotti 1995) (Figure 1*e*).

Heinrich (H) events were identified as prominent layers of ice-rafted debris in North Atlantic sediment cores (Heinrich 1988) (Figure 1*d*). Six events were originally identified over the most recent 100,000 years (H1 to H6 with increasing age); another is possible at the YD (H0; Andrews et al 1994). Most studies have focused on the more recent ones (H1 to H3 or H4). Of these, H3 (Gwiazda et al 1996a) and possibly H6 may have been somewhat anomalous.

The H layers in the Atlantic thicken towards Hudson Strait, from typically less than 1 cm in the eastern Atlantic to more than 50 cm near the strait (Andrews & Tedesco 1992, Grousset et al 1993, Andrews et al 1994). With the probable exceptions of H3 and perhaps H6, the thicker parts of these layers were deposited with greatly enhanced rates of sedimentation compared to times between H events (by perhaps an order of magnitude or more; Bond et al 1992, McManus et al 1998). Ice-rafted sediment from widespread sources around the north Atlantic is present in the thin edges of the H layers far away from Hudson Strait (Bond & Lotti 1995, Revel et al 1996) and in H3, but the thick regions of H1, H2, and H4 are dominated by material with composition indicating a Hudson Strait/Hudson Bay source region, based on data such as Pb isotopes in feldspars (Gwiazda et al 1996a), Ar-Ar dates of amphiboles (Gwiazda et al 1996b), Sm-Nd isotope systematics (Grousset et al 1993), and carbonate lithologies (Bond et al 1992).

The mass flux of ice-rafted debris in H layers thus appears to have been almost entirely dominated by Hudson Bay-area sources, although increased ice rafting did occur from other sources. The ice-rafted-debris signal from multiple ice sheets may be explained by enhanced survival of icebergs in a cold ocean, by advance of small ice sheets related to cooling, or by other processes (McCabe & Clark 1998), but the much larger sediment flux with Hudson Bay

affinity seems to require major changes in the Laurentide ice sheet in Hudson Bay/Strait (Alley & MacAyeal 1994).

The H events occurred with increased turbidite activity in the Northeast Atlantic Mid-Ocean Channel (NAMOC) (Stoner et al 1996, Hesse & Khodabakhsh 1998), which likely was caused by ice-sheet advance onto the outer continental shelf to trigger failures (Mulder & Moran 1995). Although circumstantial, this evidence further strengthens the argument for advance of Laurentide grounded ice during the H events.

The H events are correlated with especially cold times in the North Atlantic. The Heinrich-Bond (H-B) variability has been proposed to consist of cooling over a few millennia achieved by successively colder millennial D-O oscillations, followed by an H event during the cold phase of a D-O oscillation and then rapid warming (Bond et al 1993). The available data seem to indicate that the cooling of the ocean and reduction in deepwater formation preceded H events significantly (by centuries to 1 to 2 millennia? see Bond et al 1993, Zahn et al 1997), and that resumption of deepwater formation may have lagged the termination of enhanced ice-rafted-debris sedimentation (Zahn et al 1997).

MacAyeal (1993) proposed that the H events were surges from the Laurentide ice sheet in the Hudson Bay region through Hudson Strait, in response to a thermal oscillation. Thickening of ice over a frozen bed insulates that bed from the cold surface, and the reduction in snow accumulation associated with thickening leads to reduced vertical ice flow and so less cooling of the bed by the downward-moving, cold surface ice. The bed then thaws, allowing rapid ice motion that could have supplied debris-laden (Alley & MacAyeal 1994) bergs to the North Atlantic. Thinning from rapid ice motion brings cold surface ice near the bed, causing freezing and a cessation of rapid motion. The ice flow is then unable to evacuate the snow accumulation, causing the ice to thicken until thawing occurs again. A periodic oscillation results—quasi-periodic if boundary conditions are allowed to vary.

Subsequent work has demonstrated that it is very difficult to explain the H layers based on penetration of surface forcing through the Laurentide ice sheet to affect the bed (e.g. Oerlemans 1993). An ice-shelf mechanism has been invoked, involving debris "packaging" by basal freeze-on driven by shelf thickness gradients, but such a mechanism would probably have produced a different mix of sediment sources than observed (Hulbe 1997). More sophisticated modeling confirms the possibility of a thermally oscillating ice sheet in Hudson Bay (Marshall & Clarke 1997), although with somewhat smaller ice velocities and fluxes than in the MacAyeal (1993) model. Available evidence, although not conclusive, continues to be most consistent with the model that H events involved surging of the Laurentide ice sheet through Hudson Strait.

The phasing of cooling preceding H events is of considerable interest (Bond et al 1993, Zahn et al 1997). If the D-O and H-B oscillations were decoupled, it would be unlikely for the H events to have always occurred during the cold phases of the faster oscillation. This observation raises the possibility that the ice-sheet surges were triggered by D-O cooling or some process associated with that cooling. H events may have occurred during the first cold phase of the D-O oscillation following thawing of the ice sheet in Hudson Bay. A trigger might have involved marine instability (Weertman 1974), thermal state of the marginal regions (Alley et al 1996), or some ice-shelf process. Marginal regions with short response times must have been involved to have allowed triggering in centuries to a millennium or two, as observed.

Large oscillations of the southern margin of the Laurentide ice sheet occurred at about the time of, and possibly related to, H-B oscillations (Clark 1994, Mooers & Lehr 1997), probably because of the cooling. The H events are associated with the cold phase of the D-O oscillation, and so with cold and fresh surface-water conditions (Bond et al 1992, Maslin et al 1995, Cortijo et al 1997), reduced deepwater formation in the North Atlantic (Keigwin & Lehman 1994, Vidal et al 1997, Zahn et al 1997), and large climate changes in and beyond the immediate North Atlantic basin (Figure 1) (e.g. Grimm et al 1993; Clark & Bartlein 1995; Lowell et al 1995; Porter & An 1995; Benson et al 1996, 1998; Charles et al 1996; McIntyre & Molfino 1996; Phillips et al 1996; Little et al 1997; Curry & Oppo 1997; Lund & Mix 1998; Schulz et al 1998). Because of the role of NADW in H-B and D-O variability, we next review North Atlantic changes.

North Atlantic Surface-Water Hydrology and Deep Circulation

Milankovitch, H-B, and D-O variability are all linked to changes in oceanic circulation centered on the North Atlantic. Relevant paleoceanographic data suggest that the ocean has exhibited three fundamental modes of behavior during the deglaciation (Figure 2) (cf. Sarnthein et al 1994, Stocker 1998): modern (vigorous NADW formation in high-latitude seas that warms Northern Europe and Greenland greatly), glacial (less vigorous but active NADW formation, but not sinking as deeply, and occurring at lower latitudes with less warming of Greenland and Northern Europe; this may be the mode for the cold phases of non-H D-O oscillations), and Heinrich (greatly reduced NADW formation). (Sarnthein et al called this third mode "meltwater," but we chose a different name because many meltwater events apparently did not trigger it.) The modern (labeled as such in Figure 2) and glacial states (in Figure 2, time slice 21.2 cal kyear) can be compared to the two-pump and one-pump modes of Imbrie et al (1992, 1993), with the Heinrich mode (in Figure 2, time slice 15.8 cal kyear)

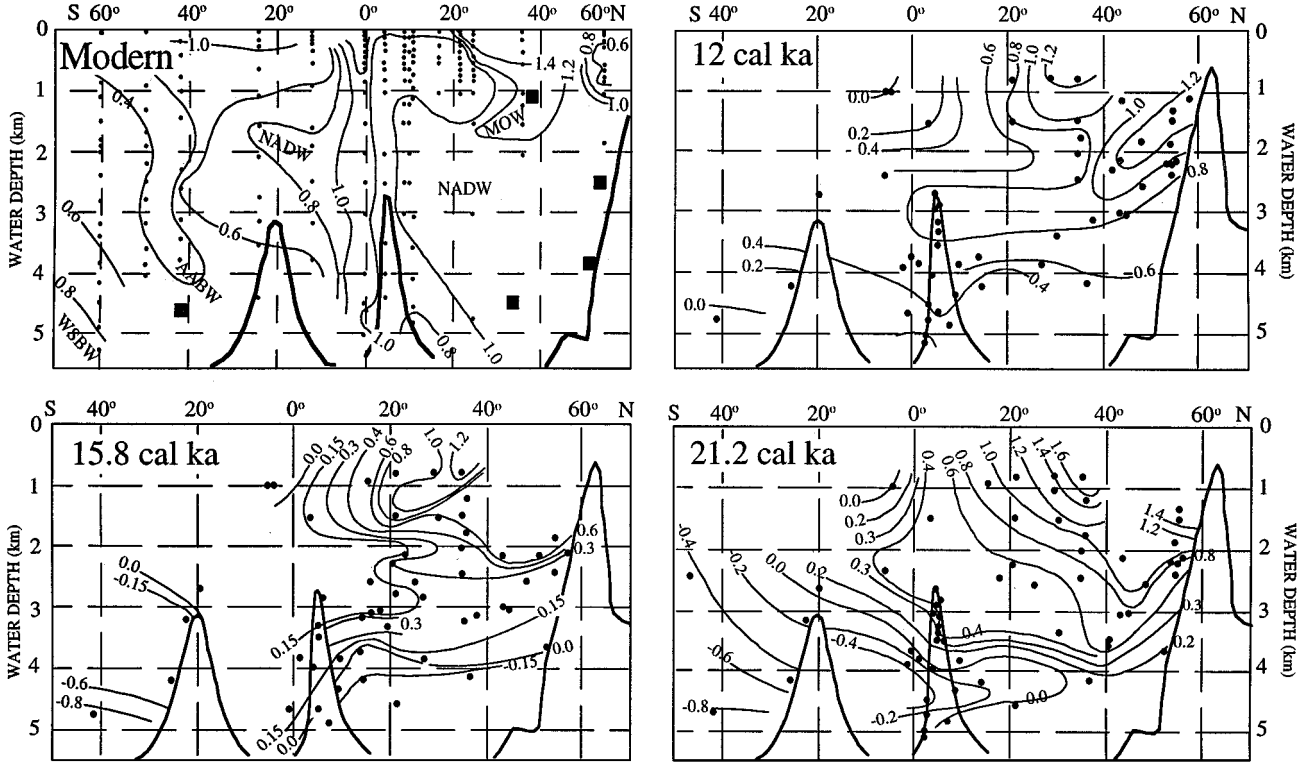

Figure 2 Distribution of $\delta^{13}C$ in the eastern Atlantic basin for four time slices: modern, 12 cal kyear, 15.8 cal kyear (Heinrich mode), and 21.2 cal kyear (glacial mode) (from Sarnthein et al 1994). *Black squares* indicate the locations of core sites with high-resolution records shown in Figure 4. Modern nutrient-depleted Mediterranean outflow water (MOW) is characterized by the highest $\delta^{13}C$ values measured on the total dissolved CO_2, North Atlantic deep water (NADW) is characterized by intermediate $\delta^{13}C$ values, and nutrient-enriched Antarctic bottom water (AABW) is characterized by the lowest $\delta^{13}C$ values. None of the $\delta^{13}C$ records are corrected for the glacial-interglacial difference.

operating at time scales shorter than those considered by Imbrie et al. Gradations, intermediates, or other modes may exist, but large jumps over years to decades have occurred between modes. As discussed below, the atmospheric effects probably have been largest in transition from modern to glacial, and the deep-ocean effects probably have been largest in transition from glacial to Heinrich, with implications for their transmission to other regions.

High-resolution geochemical records from the North Atlantic and Nordic Seas identify significant geographic and temporal variability in surface-water hydrology—sea-surface temperatures (SSTs) and sea-surface salinities (SSS)—and deep-ocean circulation during the last deglaciation, which can be linked to changes in sea-surface and air temperatures. Changes in δ^{18}O (Figure 3) represent episodic injection of icebergs and meltwater (Jones & Keigwin 1988, Lehman et al 1991, Keigwin et al 1991), varying rates of advection associated with deepwater formation (Duplessy et al 1992, Fairbanks et al 1992), and

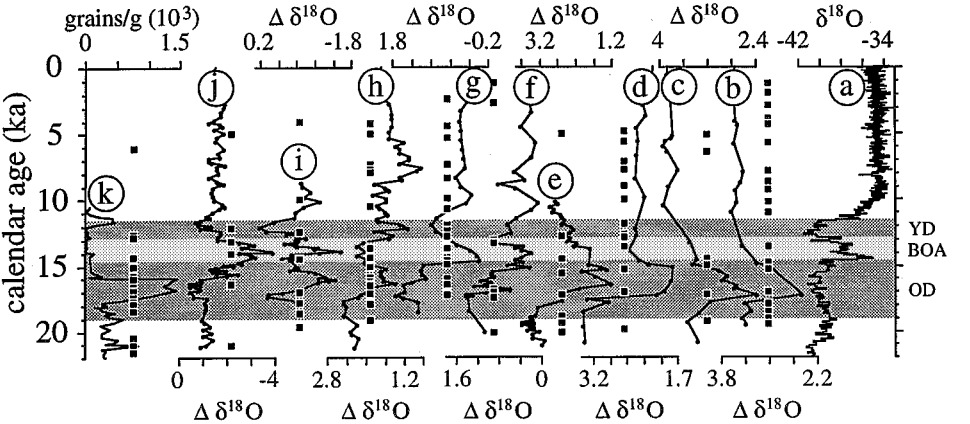

Figure 3 High-resolution North Atlantic planktonic $\Delta\delta^{18}$O records (*b–j*) (all values in per mil) compared to (*a*) the GISP2 δ^{18}O record (in per mil) (Grootes et al 1993) and (*k*) the lithic-grain record from North Atlantic core VM23-081 (Bond & Lotti 1995). We have subtracted the global ice volume component (derived from the Barbados sea-level record, Fairbanks 1989) from the δ^{18}O records in order to illustrate anomalies ($\Delta\delta^{18}$O) that reflect some combination of changes in sea-surface salinity and temperature. *Gray-scale horizontal bars* indicate the Oldest Dryas (OD), Bølling-Allerød (BOA), and Younger Dryas (YD) intervals. *Small black squares* show location of AMS radiocarbon ages in each core. Radiocarbon timescales were converted to calendar years using the relation of Bard et al (1997). Core records are: (*b*) PS21295-4 (Jones & Keigwin 1988), (*c*) HM94-34 (Koç & Jansen 1994), (*d*) V28-14 (Lehman et al 1991), (*e*) ODP 609 (Bond et al 1993), (*f*) CHN82-20 (Keigwin & Lehman 1994), (*g*) SU81-18 (Bard et al 1987), (*h*) stacked δ^{18}O records from continental slope of Nova Scotia (Keigwin & Jones 1995), (*i*) KNR31 GPC5 (Keigwin et al., 1991), (*j*) EN32 PC-6 (Keigwin et al 1991).

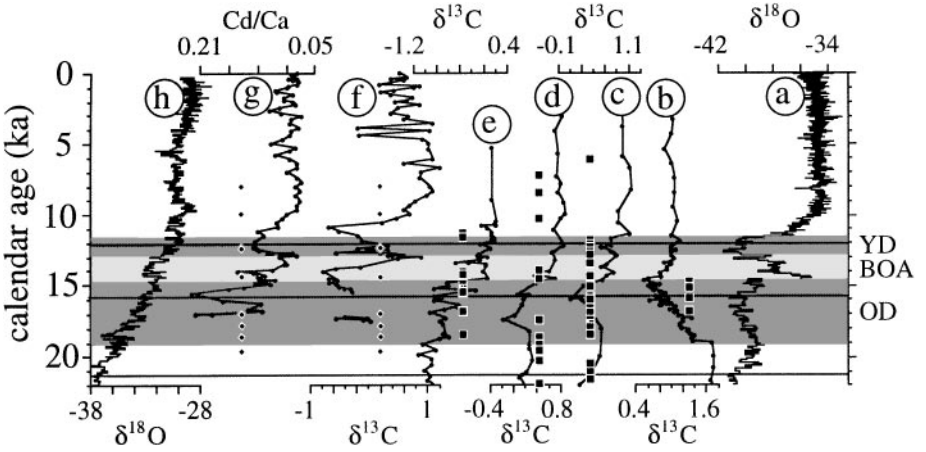

Figure 4 High-resolution nutrient records (δ^{13}C in per mil and Cd/Ca in μmole/mole) (*b–j*) spanning the last deglaciation, compared to the (*a*) GISP2 (Grootes et al 1993) and (*h*) Byrd (Sowers & Bender 1995) δ^{18}O records (in per mil). *Gray-scale horizontal bars* indicate the Oldest Dryas (OD), Bølling-Allerød (BOA), and Younger Dryas (YD) intervals. *Small black squares and diamonds* show location of AMS radiocarbon ages in each core. The *three solid horizontal lines* correspond to the time slices shown in Figure 2. Age model for core EN120-GGC1 (*f, g*) is based on graphic correlation to nearby core KNR31 GPC5 (Keigwin et al 1991), with AMS ages shown as *black diamonds* being from GPC5. Radiocarbon timescales were converted to calendar years using the relation of Bard et al (1997). The nutrient records are arranged from shallowest (1099 m) to deepest (4450 m) sites (see also Figure 2), and are thus sampling temporal variability across a depth transect of intermediate to deep waters of the North Atlantic. Core records are: (*b*) S075-26KL (1099 m) (Zahn et al 1997), (*c*) V23-081 (2393 m) (Jansen & Veum 1990), (*d*) 17045 (3663 m) (Sarnthein et al 1994), (*e*) RC11-83 (4718 m, South Atlantic) (Charles & Fairbanks 1992), (*f, g*) EN120-GGC1 (4450 m) (Keigwin et al 1991).

changes in precipitation minus evaporation (Duplessy et al 1992), with meltwater and precipitation having light isotopes. Geochemical tracers of deep-ocean nutrient distributions, primarily δ^{13}C but also Cd/Ca, monitor past variations in deepwater circulation (Figures 2, 4) (Boyle & Keigwin 1982, 1987; Curry & Lohmann 1983). Surface-water productivity strips from the water isotopically light carbon, and nutrients including phosphate and Cd (which follows phosphate). The carbon and nutrients accumulate in deep water over time through dissolution of sinking organic matter. Newly formed deep waters thus have low Cd and high δ^{13}C. Over time, Cd increases and δ^{13}C decreases.

We first compare glacial maximum to modern conditions, and then consider further changes during abrupt events. For the last glacial maximum, the δ^{13}C records show that a northward-flowing nutrient-rich water mass replaced the nutrient-poor lower NADW that now fills the deep northern and tropical Atlantic

(Figures 2, 4) (Sarnthein et al 1994, Beveridge et al 1995). A strong gradient at about 3500 m separated this nutrient-rich water mass from nutrient-poor "embryonic" NADW (Sarnthein et al 1994), which ventilated the intermediate and upper deep glacial North Atlantic and can be traced as far as 10°S (Figure 2). Finally, the most positive δ^{13}C values of this interval (>1.2 per mil) identify Mediterranean Outflow Water (MOW) at shallow water depths (<1500 m) between 20° and 40°N. This water mass persisted throughout the last deglaciation (Sarnthein et al 1994) (Figure 2).

Sea-surface salinity and temperature estimates from δ^{18}O records (Figure 3) suggest that some glacial-maximum convection occurred in the Nordic Seas, where seasonally ice-free waters existed (Weinelt et al 1996), but that most North Atlantic intermediate water (NAIW) and deep water (NADW) formed by open-ocean convection somewhere in the subpolar North Atlantic, probably south of Iceland and in the northwest (Duplessy et al 1992, Labeyrie et al 1992, Oppo & Lehman 1993, Sarnthein et al 1995, Weinelt et al 1996). Ventilation rates of NADW (or NADW+NAIW) were similar to today's rates, although higher fluxes characterized intermediate waters and lower fluxes occurred at depth (Oppo & Lehman 1993, Boyle 1995). Recent ^{231}Pa/^{230}Th data support the notion of a glacial NADW forming at near-modern rates and feeding waters of the Southern Ocean (Yu et al 1996).

Little change occurred in the δ^{13}C values of the eastern Atlantic basin between the last glacial maximum ~18 ^{14}C kyear (thousand radiocarbon years before present) (21 cal kyear) and 15.5 ^{14}C kyear (18.3 cal kyear), suggesting that glacial NADW continued to form in similar fashion throughout this interval, although the site(s) of convection may have shifted slightly (Sarnthein et al 1994). Geochemical data suggest a major change in North Atlantic surface-water hydrology and intermediate and deep-ocean circulation starting at 15.5–16 ^{14}C kyear (18.3–19 cal kyear), which is the start of the cooling often identified with the Oldest Dryas and leading to H1 and the "Heinrich" state of ocean circulation. North Atlantic and Nordic Sea δ^{18}O records indicate a widespread low-salinity event during the Oldest Dryas (Figure 3). Estimates of North Atlantic SST and SSS indicate that surface-water densities were too low to form intermediate or deep water during this interval (Sarnthein et al 1995, Maslin et al 1995, Labeyrie et al 1995).

Within the Nordic Seas (Figures 3*b*, *c*, *d*), this distinct event, which Sarnthein et al (1995) identify as the largest excursion of the last 60 kyear, is thought to represent the first major retreat of marine margins of the Barents and Fennoscandian ice sheets (Jones & Keigwin 1988, Lehman et al 1991). Discharge of icebergs from the Laurentide, Icelandic, and Greenland Ice Sheet during H1 (Figure 3*k*) (Bond & Lotti 1995), which accompanied this event, likely accounts for the δ^{18}O minima seen in cores extending across the subpolar North Atlantic

(Figures 3*e*, 3*f*, 3*h*) and possibly as far south as the Bermuda Rise (Figure 3*i*). Cold, low-salinity surface waters are also registered off the Portugal coast (Figure 3*g*) (Bard et al 1987, Duplessy et al 1992).

Oldest Dryas δ^{13}C and Cd/Ca reached the most extreme values characteristic of nutrient enrichment of any time during the last deglaciation (Figure 4). This nutrient distribution at 13.5 ^{14}C kyear (15.8 cal kyear) clearly signals: (*1*) a shutdown of NADW formation, (*2*) reduced NAIW formation, and (*3*) southward flow of NAIW, which did not extend beyond the equator (Sarnthein et al 1994) (Figure 2).

At the onset of the Bølling-Allerød warm interval, δ^{18}O values increased throughout the Nordic Seas (Figures 3*b*, 3*c*, 3*d*) and the NE North Atlantic (Figure 3*e*), and showed no significant variability through the remainder of the deglaciation although some high-resolution records in the North Sea suggest meltwater influences associated with drainage of the Baltic Lake late in the deglaciation (Lehman & Keigwin 1992b, Boden et al 1997). Elsewhere in the North Atlantic, SST records (Bond & Lotti 1995, Sarnthein et al 1995) indicate that sea-surface warming was primarily responsible for the δ^{18}O minimum recorded during the Bølling-Allerød interval. In conjunction with increased warm-water planktonic foraminifera, the δ^{18}O maximum recorded off Nova Scotia indicates increased salinity (Figure 3*h*) (Keigwin & Jones 1995), whereas the large decrease in δ^{18}O values ($\sim$4 per mil) from the Gulf of Mexico reflects increased melting from the Laurentide Ice Sheet (Figure 3*j*) (Clark et al 1996). Nutrient levels during this time changed to values comparable to interglacial values (Figure 4), suggesting the establishment of a deep-ocean circulation in the North Atlantic similar to modern circulation, with only small-scale variability.

Only the records off Nova Scotia (Keigwin & Jones 1995, de Vernal et al 1996) (Figure 3*h*) suggest a significant δ^{18}O anomaly during the YD, which is consistent with the known routing of Lake Agassiz waters from the Mississippi to the St. Lawrence River at this time (Teller 1990). This routing event is also well expressed in the Gulf of Mexico δ^{18}O record (Broecker et al 1988, Clark et al 1996). Because only cores monitoring the deepest waters in the western North Atlantic basin (Boyle & Keigwin 1987, Keigwin et al 1991) show a significant change in nutrients during the YD (Figures 4*f*, 4*g*), some controversy has existed regarding the extent of change in deep-ocean circulation at this time (Jansen & Veum 1990, Veum et al 1992, Lehman & Keigwin 1992a, 1992b, Boyle 1995). The balance of evidence suggests a western deep-water response, with no signals or smaller signals in shallower and eastern deep waters (Figures 4*b*, 4*c*, 4*d*, Figure 2: 12 cal kyear), either because the change was restricted to western deep waters or because low sedimentation rate and bioturbation have combined to remove the signal in other records (Lehman & Keigwin 1992a, Boyle 1995).

For records older than H1, high-resolution coverage is less common, and orbital variations complicate interpretation. Nonetheless, other H events seem to have had a similar effect on the ocean as H1 had (especially H2, H4, and H5; H3 and perhaps H6 seem "smaller" or otherwise anomalous). The record of Zahn et al (1997) is long enough to capture H4 and shows great reduction in NAIW at H2 and H4 as well as at H1. Sarnthein et al (1994) have records across H2, and interpreted NADW weakening at about the age of H2 (Figure 21 in Sarnthein et al 1994). At a site sampling modern NADW, Oppo & Lehman (1995) found a strong carbon-isotopic signature of reduced NADW formation at H5, as well as for younger H events and cold phases of D-O oscillations. Maslin et al (1995) reconstructed sea-surface conditions in the northeast Atlantic from just preceding H4 to the present. They found that H1-H4 were times of cold and especially low salinity, with more effect on surface-water salinity than for other D-O stadials. Maslin et al also found evidence for a three-step pattern of warm, almost-modern conditions just after an H event, then glacial conditions, and then Heinrich conditions.

Rasmussen et al (1996) reconstructed deep-water outflow from the Nordic seas in a core covering H1-H5. They found strong outflow correlated with warm times, transitional intervals between warm and cold conditions, and little or no outflow during each of the cold D-O stadials. Interestingly, one of their key indicators shows a much stronger response to H1-H5 than to other D-O stadials (last panel of Figure 5 in Rasmussen et al 1996).

Strong oscillations can be produced in models of the ocean thermohaline circulation (e.g. Broecker et al 1990, Birchfield & Broecker 1990, Sakai & Peltier 1995). Deep-water formation in the north Atlantic is linked to cooling of initially high-salinity waters. Freshwater dilution of these waters can reduce their salinity sufficiently to prevent deep-water formation, reducing the oceanic heat flux to high northern latitudes and triggering other climatic changes. An oscillator can be modeled in which deep-water formation leads to ice-sheet melting, increased freshwater supply, and deep-water reduction or shutdown, followed by ice-sheet growth, ocean-salinity increase, and resumption of deep-water formation. "Preconditioning" of the North Atlantic with freshwater may cause deep-water formation to become "inherently unstable" (Tziperman 1997; also see Sakai & Peltier 1995), such that it may rapidly strengthen, collapse, or oscillate.

Of course, the ability to model such a signal does not mean that the cause has been identified. Perhaps it is related to solar variability or other processes, although large solar changes are unlikely, based on cosmogenic isotopes in ice cores (e.g. Finkel & Nishiizumi 1997, Lal et al 1997). Similarity between the D-O frequency and the characteristic timescale for deep-ocean circulation supports a role for the thermohaline circulation. We next review evidence strengthening this relation.

Rates and Routings of Meltwater Flux to the North Atlantic

Broecker et al (1988, 1989) first suggested that the well-dated change in routing of meltwater from the Mississippi to the St. Lawrence River 11 ^{14}C kyear, followed by rerouting of these waters down the Mississippi at 10 ^{14}C kyear, was responsible for a reduction in NADW formation and the YD cooling. In light of the Barbados sea-level record (Figure 5*b*) (Fairbanks 1989), and considering that meltwater-routing could not explain each of the earlier D-O events, Broecker et al (1990) proposed the salt oscillator (see above), and relegated the meltwater routing hypothesis to a secondary forcing that triggered the YD through its effect on an already sluggish NADW weakened by the preceding meltwater pulse-1A (mwp-IA).

Clark et al (1996) argued that evidence identifying the origin of and response to mwp-IA was elusive. Given that much smaller meltwater events have clearly left their signal in North Atlantic records (Figure 3), it is somewhat surprising that an event the size of mwp-IA (order of 0.5 Sv $= 0.5 \times 10^6$ m^3 s over 300–500 years) should go largely unnoticed. Lehman et al (1993) suggested that advection and downwelling of low-salinity surface waters in an actively running "conveyor belt" may result in the loss of a planktonic foraminiferal δ^{18}O signal. However, most ocean models predict that thermohaline circulation would decrease rapidly and dramatically in response to a freshwater forcing the magnitude of mwp-IA (Maier-Raimer & Mikolajewicz 1989, Stocker et al 1992, Stocker & Wright 1996, Rahmstorf 1995, Mikolajewicz et al 1997, Manabe & Stouffer 1997), and thus not be able to advect the signal from North Atlantic surface waters. The timescale of modeled response (order of 100 years) is much shorter than the thousand-year interval between mwp-IA and the YD, whereas the magnitude and duration of the modeled response are much larger than the Intra-Bølling Cold Period (IBCP), which occurred at the same time as mwp-IA (Figure 5) (Bard et al 1996, Clark et al 1996).

Thus we are left with an apparently very large forcing (mwp-IA) coincident with a minor response (IBCP) versus a much smaller forcing (meltwater routing to the St. Lawrence) coincident with a large response (YD). In view of these issues, we consider the origin and impact of mwp-IA to remain an unresolved but critical question in understanding the dynamics of the last deglaciation.

If the meltwater-routing event through the St. Lawrence River 11-10 ^{14}C kyear was responsible for the YD cooling, other meltwater-routing events may have similarly affected North Atlantic climate. To evaluate this hypothesis, we compare the meltwater-routing history of the southern margin of the Laurentide Ice Sheet to high-resolution climate records of the last deglaciation (Figure 5). Ocean models predict a greater deep-water response to Laurentide meltwater delivered to the North Atlantic from eastern outlets (Hudson River,

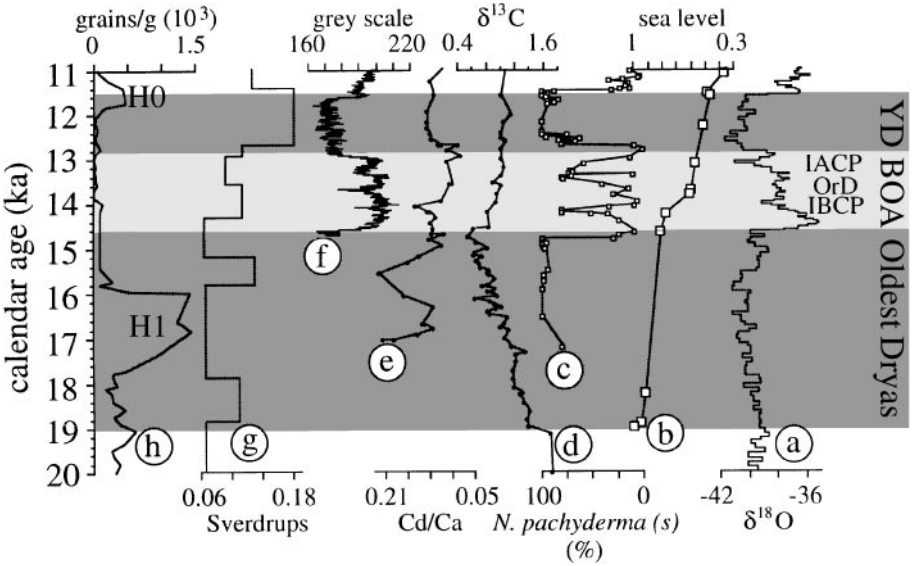

Figure 5 Climate records of the last deglaciation (*a–f*) compared to records of freshwater flux to the North Atlantic (*g, h*). (*a*) GISP2 δ^{18}O record (in per mil) (Grootes et al 1993), (*b*) Barbados sea-level record (normalized) (Fairbanks 1989), (*c*) percentage of *Neogloboquadrina pachyderma* (s.) from North Atlantic core Troll 8903 (Haflidason et al 1995), (*d*) δ^{13}C record from core S075-26KL (Zahn et al 1997), (*e*) Cd/Ca record from core EN120-GGC1 (Keigwin et al 1991), (*f*) Cariaco basin grey-scale record (Hughen et al 1996), (*g*), freshwater fluxes routed through the Hudson and St. Lawrence rivers (Teller et al 1998), and (*h*) concentrations of lithic grains from core V23-081 (Bond & Lotti 1995). *Gray-scale horizontal bars* indicate the Oldest Dryas (OD), Bølling-Allerød (BOA), and Younger Dryas (YD) intervals. We constructed the age model for Troll 8903 by linear interpolation between AMS radiocarbon ages, after subtracting 800 years. This correction gave the best age agreement with subtropical (Bard et al 1987) and tropical (Hughen et al 1996) radiocarbon dated records (with 400-year reservoir correction) for age of onset of the Bølling and Younger Dryas intervals, suggesting an 800-year reservoir correction for high-latitude North Atlantic sites may apply for the Bølling-Allerød interval as well as the Younger Dryas (Bard et al 1994). We have calibrated radiocarbon-dated records using the relation in Bard et al (1997). We used the radiocarbon-dated Cariaco Basin grey-scale record, which on a calendar year timescale is in phase with the GISP2 record (Hughen et al. 1996), to directly compare the radiocarbon ages of land and marine records with the calendar ages of the three centennial-scale climate events that occurred during the Bølling-Allerod interval (the intra-Bølling cold period (IBCP), the Older Dryas (OrD), and the intra-Allerød cold period (IACP) in the GISP2 record.

St. Lawrence River) than from the southern outlet (Mississippi River) (Maier-Raimer & Mikolajewicz 1989, Manabe & Stouffer 1997), and that preconditioning of North Atlantic surface waters by meltwater delivered through the southern outlet may be important in increasing sensitivity to meltwater subsequently routed through the eastern outlets (Fanning & Weaver 1997). To test the meltwater-routing hypothesis, identifying the timing of the opening of these outlets and the meltwater flux through them is required.

Teller (1990) first quantified these amounts for the interval surrounding the YD (12-9 ^{14}C kyear). Teller et al (1998) revised these calculations and extended them over the entire deglaciation. In general, they found (Figure 5) that when retreat of the Laurentide ice margin during interstadials uncovered an eastern outlet (the Hudson and, subsequently, St. Lawrence Rivers), the eastward freshwater flux increased, and North Atlantic climate cooled. When readvance of the ice margin closed off the eastern outlet, the eastward freshwater flux decreased and climate warmed.

The Oldest Dryas interval is a composite of successive freshwater forcings, beginning with eastward routing, followed by icebergs from H1 and then followed by eastward routing (Figure 5). While the onset of the IACP at $\sim$11.5 ^{14}C kyear is associated with little change in magnitude of freshwater supply to the North Atlantic, it is associated with a shift in routing from the Hudson River to the St. Lawrence River. Because the St. Lawrence River routing would deliver freshwater directly to the Labrador Sea, this routing likely had a greater effect on North Atlantic salinities than routing through the Hudson River, in the same fashion that ocean models distinguish a greater response to St. Lawrence versus Mississippi routing (Manabe & Stouffer 1997).

The excellent agreement between the timing of meltwater routing or iceberg discharge events and climate change in the North Atlantic during the last deglaciation (Figure 5) supports the notion that freshwater forcing of NAIW/NADW played a key role in driving centennial- to millennial-scale climate change during the last deglaciation. The interplay between routing events and North Atlantic climate change suggests a possible feedback mechanism explaining the rapid and abrupt ice-marginal oscillations along the southern Laurentide margin superimposed on general margin retreat of the last deglaciation (Clark 1994); in addition, a similar oscillatory system may have existed at other times when the southern margin was at these latitudes.

However, we do not suggest that a routing mechanism was responsible for earlier D-O events, particularly during marine isotope stage 3. We believe instead that the significance of the meltwater-routing hypothesis is in identifying the sensitivity of the thermohaline circulation to freshwater forcing under a range of conditions. It is possible that the ocean oscillates freely at 1500 years or somewhat longer (e.g. Bond et al 1997), and that as the system approaches

the threshold for a spontaneous mode switch, progressively smaller forcing is capable of triggering a mode switch (Rahmstorf 1995). If this is so, then in a variable system all mode switches will be triggered, but timing as well as magnitude of forcing will be significant in effectiveness. Such variable effectiveness of forcing may have played some role in apparent mismatches between forcing and response magnitudes during the deglaciation, discussed above.

N-S Phasing

As noted above, climate changes for much of the Earth seem to have been similar to those in the North Atlantic region, with a cold North Atlantic correlated to generally cold, dry, or windy conditions elsewhere. Whereas this correlation appears to be global at Milankovitch frequencies, it is widespread but not global at D-O frequencies, and has some out-of-phase regions at H-B frequencies.

To further evaluate this, we compare high-resolution marine and ice-core records from the Southern Hemisphere spanning the last deglaciation (Figures 6, 7). More and better-dated records are needed from some regions; we summarize many of the best records here.

These records suggest two different responses, which Bender (1998) refers to as a "northern" and "southern" response. The northern response shows the same signature of abrupt climate changes during the last deglaciation as seen in Greenland ice-core records, whereas in the southern response warming following the last glacial maximum is interrupted by the Antarctic Cold Reversal (ACR) between ~13 to 15 cal kyear (Figure 6) (Jouzel et al 1995, Sowers & Bender 1995). Alternately, one might view the southern response as one of anomalously rapid warming at the time of H1, with the ACR a return to "normal" deglaciation.

Well-dated time series of the northern response are represented by records of sea-surface temperatures (SSTs) in the Indian Ocean east of southern Africa (Figures 6, 7) (Labracherie et al 1989, Pichon et al 1992, Bard et al 1997). In particular, these records show abrupt warming at the onset of the Bølling-Allerød period, and a small cooling during the YD. The δ^{18}O signal in core MD84-527 (Figure 6*e*) (Labracherie et al 1989) suggests some combination of an abrupt increase in temperature and decrease in salinity at the onset of the Bølling, and a reversal during the YD, whereas summer SSTs estimated from transfer functions (Figure 6*d*) (Pichon et al 1992) suggest more gradual warming, beginning with the onset of the Bølling and culminating with abrupt warming at the end of the YD. Records of monsoonal variations in the Arabian Sea show enhanced (weaker) monsoons during Greenland interstadials (stadials) (Sirocko et al 1996, Schulz et al 1998), suggesting a broad region directly east of the African continent with the characteristic structure of the northern response.

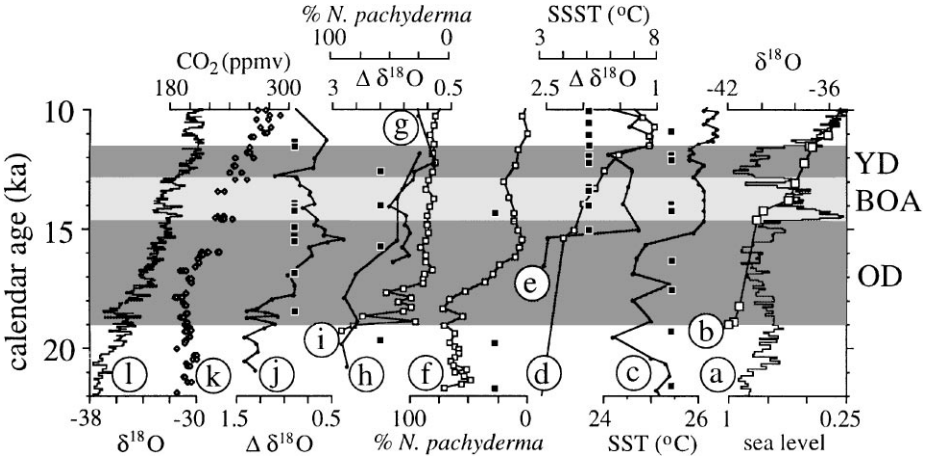

Figure 6 High-resolution records from the southern hemisphere (*c*–*l*) compared to (*a*) the GISP2 δ^{18}O record (in per mil) (Grootes et al 1993) and (*b*) the Barbados sea-level record (normalized) (Fairbanks 1989) (see Figure 7 for location of records). We have subtracted the global ice volume component (derived from the Barbados sea-level record; Fairbanks 1989) from the planktonic δ^{18}O records in order to illustrate anomalies ($\Delta\delta^{18}$O) which reflect some combination of changes in sea-surface salinity and temperature. *Gray-scale horizontal bars* indicate the Oldest Dryas (OD), Bølling-Allerød (BOA), and Younger Dryas (YD) intervals. *Small black squares* show location of AMS radiocarbon ages in each core. The records are: (*c*) alkenone-derived sea-surface temperature (SST) estimates from MD 79257 (Bard et al 1997), (*d*) summer sea-surface temperature (SSST) estimates and (*e*) $\Delta\delta^{18}$O record (in per mil) from core MD 84 527 (Labracherie et al 1989; Pichon et al 1992), (*f*) percentage of *Neogloboquadrina pachyderma* (s.) from core GeoB 1711 (Little et al 1997), (*g*) $\Delta\delta^{18}$O record (in per mil) measured on *Globigerina bulloides*, (*h*) $\Delta\delta^{18}$O record (in per mil) measured on *Neogloboquadrina pachyderma* (s.), and (*i*) percentage of *Neogloboquadrina pachyderma* (s.) from core MD88-770 (Labeyrie et al 1996), (*j*) $\Delta\delta^{18}$O record (in per mil) from core RC11-83 (Charles et al 1996), (*k*) atmospheric CO_2 record from the Byrd core (Sowers & Bender 1995), and (*l*) δ^{18}O record (in per mil) from the Bryd core (Sowers & Bender 1995).

Other records (not shown) with a northern response include those of mountain-glacier advances in South America and New Zealand (Figure 7) during the Oldest Dryas (H1) and the YD, respectively (Denton & Hendy 1994, Lowell et al 1995). Finally, the ice-core record from Taylor Dome, Antarctica also shows the northern response (Mayewski et al 1996, Bender 1998, Steig et al 1998).

Records showing the southern response include other Antarctic ice cores (e.g. Jouzel et al 1995). Using the δ^{18}O of atmospheric O_2 for correlation, Sowers & Bender (1995) placed the Byrd ice-core chronology on a common timescale with the GISP II chronology (Figure 6). Using methane, Blunier et al (1997) similarly correlated the Vostok ice-core chronology to the GRIP record. These two Antarctic ice-core records suggest that significant deglacial warming

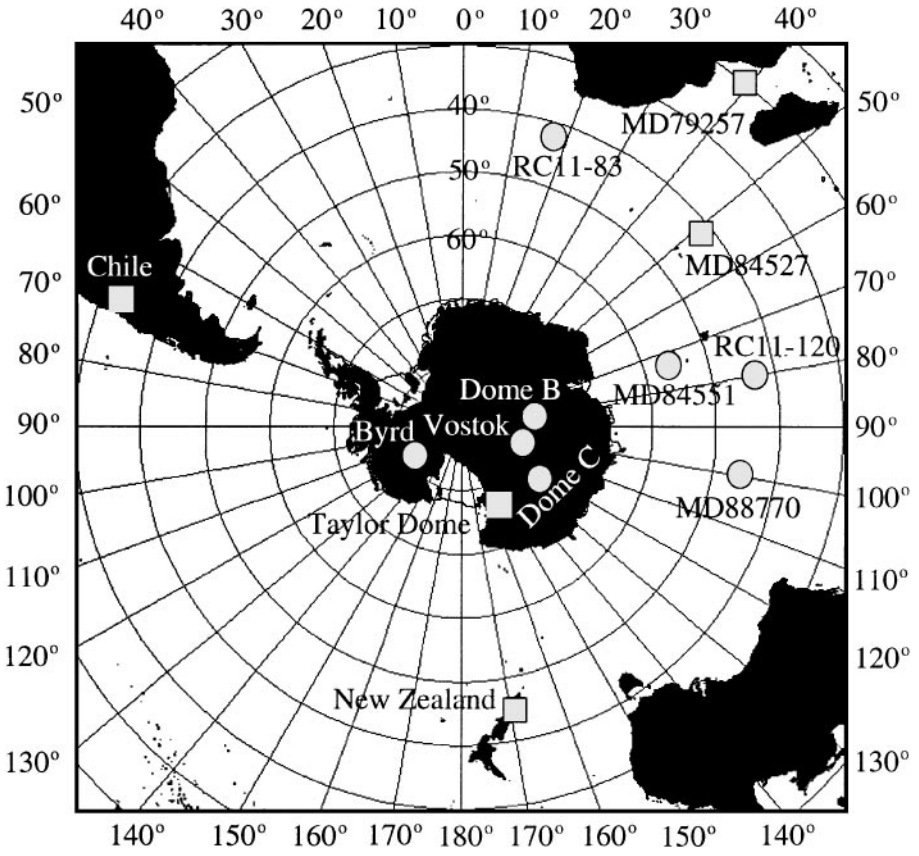

Figure 7 Map of the southern hemisphere showing distribution of sites with evidence of either a northern response (*squares*) or a southern response (*circles*) during the last deglaciation (see text for further explanation).

began between 19 and 20 cal kyear, or near the onset of Oldest Dryas cooling seen in Greenland records (Figure 6). Note that the isotopically coldest time in Greenland was 23 to 24 cal kyear (Grootes & Stuiver 1997). A consistent though not unique interpretation is that northern warming led southern warming and was nearly synchronous with northern summer insolation, but was interrupted by meltwater events (McCabe & Clark 1998). Byrd and Vostok warming continued until ~14.2 to 14.7 cal kyear, or near the onset of Bølling warming, when the ACR began. The ACR continued until ~13.6 to 13.8 cal kyear, coincident with the onset of the YD, when Antarctic temperatures warmed again, reaching their interglacial maximum by ~11.5 cal kyear.

This southern response is also present in several well-dated marine records (Figures 6, 7). Two SST records from the South Atlantic (GeoB1711 at 23°S, Figure 6*f*; RC11-83 at 41°S, Figures 6*j*, 7) and two records from the Indian Ocean (MD88770 at 45°S, Figures 6*g*, 6*h*, 6*i*, 7; MD84551 at 55°S, Figure 7) show onset of deglacial warming at the same time as for Byrd and Vostok. The *Neogloboquadrina pachyderma* record from core MD88-770 in the central Indian Ocean (Figure 6*i*) (Labeyrie et al 1996) suggests an abrupt change at the onset of deglacial warming. Insofar as the core is now situated near the Subtropical Front, the abrupt decrease in *Neogloboquadrina pachyderma* may reflect passage of this front. The SST records also suggest cooling during the ACR, followed by rapid warming (Figure 6).

The spatial variability in the distribution of the response of the Southern Hemisphere during the last deglaciation (Figure 7) is significant in identifying a mechanism or mechanisms that transmit North Atlantic climate change across the equator to produce a northern response in some regions versus other regions in which a southern response is registered. Many more data sets are needed, but it appears that the southern response is focused on the South Atlantic and the central Indian Ocean.

Imbrie et al (1992, 1993) proposed that an early response of Southern Ocean SSTs which led global ice volume changes (i.e. a southern response) resulted from an increase in the rate of formation of NADW. Because NADW is warmer than Antarctic bottom water (AABW), upwelling of NADW in the Southern Ocean followed by formation of AABW may provide heat to the Antarctic. However, drawing upon the out-of-phase climate behavior between the Byrd and GISP II records during the Bølling-Allerød-YD interval (Figure 6), Broecker (1998) proposed that a reduction (increase) in formation of NADW would be balanced by increased (decreased) convection somewhere in the Southern Ocean (Stocker & Wright 1996, Schiller et al 1997), resulting in cooling (warming) in the North Atlantic and corresponding warming (cooling) in the Southern Hemisphere. In addition, NADW formation causes water warmed in the South Atlantic to release that heat in the high northern latitudes. Reduction in NADW formation then would tend to leave that heat in the South Atlantic, warming it (Crowley 1992). Based on radiocarbon data and at least consistent with available dating of climate records, Broecker (1998) suggested that the deepwater-formation contribution to southern warming during northern cooling lags the northern cooling on the century scale.

Data in Figure 6 suggest that a southern-northern seesaw also operated during the Oldest Dryas, when significant warming in some regions of the Southern Hemisphere coincided with severely reduced rates of NADW formation (see above). Longer time series similarly show out-of-phase interhemispheric behavior between rates of NADW formation and Vostok ice isotopes and South

Atlantic SSTs (Bender et al 1994, Charles et al 1996, Little et al 1997). In long records, the southern response is especially prominent for H events and less so for non-H D-O oscillations (Bender et al 1994, Blunier et al 1998).

Similar behavior is exhibited in the North Pacific. The Santa Barbara Basin has a clear northern signal (Figure 1*g*), in which oxygenated conditions related to increased intermediate-water circulation, cooler surface conditions or stronger winds occurred during the cold phases of Atlantic D-O oscillations, with little or no time lag (Behl & Kennett 1996). However, deep Northeast Pacific waters seem to record an "anti-northern" or southern signal, in which increased ventilation is related to reduced North Atlantic ventilation (Figure 1*h*) (Lund & Mix 1998). This deep Pacific response seems to have lagged the North Atlantic changes by a few centuries for the YD (older dating is not sufficiently accurate to assess such lags), and seems to have recorded H events but missed D-O oscillations (Lund & Mix 1998). This is consistent with oceanic transmission of the southern climate-change signal from the southern ocean (Lund & Mix 1998).

The presence of a northern response in some regions of the Southern Hemisphere (Figure 7) shows that the influence of Broecker's "bipolar seesaw" mechanism is not hemispherically symmetric. Instead, the northern response suggests that the influence of changes in NADW is rapidly transmitted across the equator in some fashion to be registered directly in some regions of the Southern Hemisphere.

Manabe & Stouffer (1997) and Tziperman (1997) found from model studies that large areas of the Southern Hemisphere cooled in response to a reduced rate of NADW formation. Southern Hemisphere sites with a northern response (Figure 7) generally occur in the areas of negative temperature anomalies corresponding to "NADW off" (Manabe & Stouffer 1997).

In addition, changes in North Atlantic SSTs corresponding to changes in NADW may be transmitted across the equator as a northern signal through their influence on the African and Asian monsoon, thus explaining the data from east of Africa (Street-Perrott & Perrott 1990, Hostetler et al 1999) (Figures 6, 7). This mechanism probably is part of a more general class of processes that act to synchronize the hemispheres at orbital as well as millennial timescales, as discussed next.

N-S Orbital Synchronization

An emerging picture, which still requires more confirmation, is that the entire Earth experiences a northern response at orbital frequencies (complicated though it is by local insolation and other effects). For larger and longer-lasting millennial events (especially H events), some regions at high southern latitudes centered on the South Atlantic and into the deep Pacific experience an

anti-northern or southern response transmitted through the ocean over centuries, while the rest of the Earth has a northern response transmitted through the atmosphere with little time delay. For smaller or shorter-lived D-O oscillations, the North Atlantic and regions somewhat beyond experience a northern response, but the high southern latitudes appear to have little or no response. The out-of-phase behavior between north and south is explainable through the oceanic seesaw (Broecker 1998), but then how are the hemispheres synchronized at orbital timescales and D-O timescales?

Citing Manabe & Broccoli (1985), Broecker & Denton (1989) argued that the direct atmospheric transmission of cooling at high northern latitudes to sites at high southern latitudes is small or zero. However, using a general circulation model with mixed-layer ocean lacking thermohaline circulation, Pollard & Thompson (1997) recently showed that setting appropriately low CO_2 levels, large ice sheets, and orbital parameters for glacial-maximum conditions produces significant global cooling, including cooling at high southern latitudes. Pollard & Thompson (1997) argued further that the results of Manabe & Broccoli (1985) are consistent with these newer simulations in showing that glacial-maximum boundary conditions produce strong and more or less hemispherically symmetrical cooling, if allowance is made for the extra cooling achieved by the elevation and radiative effects of the large ice sheets that grew primarily in the north.

However, in model-data comparison for glacial-maximum conditions (Table 1 in Pollard & Thompson 1997) at 18 sites spanning all latitudes (using the accurate borehole temperature calibrated results for central Greenland), Pollard & Thompson (1997) obtained modeled temperature changes less than observed for 16 of the 18 sites, and new results from Vostok, Antarctica now show that modeled temperatures changed less than observed for this 17^{th} of the 18 sites (Salamatin et al 1998). The difference for all 18 sites as tabulated averages 2.5°C, with no latitudinal trend.

This difference can be interpreted in several ways. Perhaps the GENESIS model is not sufficiently sensitive to changes in CO_2 and ice albedo (the success of the model in many tests argues against this). Perhaps the CO_2 level chosen was not sufficiently low: as discussed by Pollard & Thompson (1997), they chose a slightly high late–glacial-maximum CO_2 level to allow comparison to recent runs with recent CO_2 because of disequilibrium between recent climates and CO_2 levels. However, we consider it more likely that there is an additional change between glacial maximum and modern, not directly related to greenhouse gases or ice sheets, that caused glacial-maximum cooling to be larger than calculated by Pollard & Thompson.

Some possibilities include changes in clouds, vegetation, and dust (again, we do not consider changes in NADW production as a likely explanation

because response to the NADW changes associated with D-O events has had little effect in much of Antarctica, and response to the further changes of H events has warmed portions of Antarctica). The strong dissimilarity between dust and temperature time series from various sites including Vostok, Antarctica (Lorius et al 1990) casts doubt on this mechanism, as does the difficulty of obtaining such a large change based on aerosols (see discussion in Pollard & Thompson 1997). The models calculate clouds. Although one cannot rule out the possibility that some significant cloud feedback has been missed, we follow Pollard and Thompson (1997) in assuming that this is not the case. In simulations using the GENESIS general circulation model and fixed sea-surface temperatures, Crowley & Baum (1997) found that vegetation feedbacks can have large regional impacts but essentially no globally averaged effect (biome-wide effects to a few degrees, continent-wide effects to a few tenths of a degree but globally averaged effects of only 0.15°).

The most likely feedback may be the oceanographic effects of the stronger winds associated with cold times (e.g. Ganopolski et al 1998, Bush & Philander 1998). Stronger winds increase mixing in the ocean, cooling the warmest regions. Because of the exponential increase of evaporation rate and equilibrium vapor pressure with temperature, mixing will tend to reduce the global atmospheric water-vapor loading, which in turn will tend to cool the planet (Broecker 1997). Ganopolski et al (1998) found that in glacial-maximum reconstructions using an intermediate-complexity ocean-atmosphere model, a switch from specified modern heat flux in a slab ocean to full ocean dynamics caused tropical cooling, strong northern cooling, but slight high-latitude southern warming. Their model also shows that tropical cooling is related to both the enhanced meridional temperature gradient and to enhanced Ekman circulation caused by stronger northern hemisphere trade winds, as well as water-vapor feedbacks. Bush & Philander (1998), in a fully coupled ocean-atmosphere GCM, similarly simulated strong ice-age tropical cooling in response to stronger winds causing stronger upwelling, mixing of cooler extratropical waters into the tropics, and associated reduction in atmospheric water vapor.

Numerous authors have presented evidence for stronger winds, and stronger tropical upwelling, during glacial times. For example, Patrick & Thunell (1997) compared oxygen-isotopic changes in surface-dwelling, thermocline-dwelling, and subthermocline-dwelling foraminifera from the eastern and western Pacific. They found glacial-maximum cooling larger than interpreted by CLIMAP reconstructions, linked to a shoaling of the thermocline in the eastern Pacific. They interpreted this as indicating the effect of increased wind-driven upwelling associated with stronger trade winds.

Pisias & Mix (1997) computed radiolarian-based empirical-orthogonal-function transfer functions for cores from the eastern equatorial Pacific. They found

greater glacial-maximum cooling than in CLIMAP, again plausibly linked to increased wind strength.

Andreasen & Revelo (1997) used factor-analyzed core-top foraminiferal abundances compared to modern hydrography to develop transfer functions that they applied to glacial-maximum samples from the equatorial Pacific. For glacial maximum, they reconstructed a steeper east-west thermocline slope than modern, suggesting stronger zonal wind stress (Walker circulation), and an equatorward compression of climate zones. They emphasized that this enhanced wind stress is unlikely to have caused major temperature changes, such as cooling of more than 3°C in the western equatorial Pacific. However, the imbalance remaining in the Pollard & Thompson (1997) simulations is $<3^{\circ}$C. Lyle (1988) documented enhanced organic carbon concentrations in glacial-age sediments in the equatorial Atlantic and Pacific. Of the several possible explanations, this is at least plausibly linked to enhanced productivity and consistent with enhanced wind-driven upwelling in glacial times.

Mix et al (1986) documented that the most significant mode of glacial-interglacial climate change in the tropical Atlantic Ocean was centered on the eastern boundary currents and tropical upwelling areas. In this hemispherically symmetrical mode of variability, cold times are taken as probably indicating stronger or more zonal trade winds.

Many Pacific records of wind-blown dust show a spectral peak at about 31 kyear (e.g. Rea 1994), which may be related to but is not a direct result of orbital forcing. The presence of a 31 kyear peak in Vostok, Antarctica isotopic (temperature) records (Yiou et al 1991) is at least consistent with an important role for tropical, wind-related processes in affecting southern temperatures. The presence of this peak also shows that the system is more complex than any simple story we tell.

Much evidence thus supports the hypothesis that stronger, and possibly more zonal, glacial-maximum trade winds enhanced vertical and/or lateral mixing, reducing tropical sea-surface temperatures. This may have been achieved by more persistent La Niña-type conditions or in other ways. However it was achieved, the dominant effect of tropical conditions on global climate would have allowed even a small tropical change to affect widespread regions. It is likely that water-vapor feedbacks (Broecker 1997, Bush & Philander 1998) were particularly important.

Such a mechanism would act at orbital, H-B, and D-O timescales. However, some of the positive feedbacks (notably ice-sheet area and atmospheric CO_2 concentration) change more slowly than the D-O timescale but change greatly on the orbital timescale. Thus the D-O climate signal should be smaller in amplitude or geographical coverage than the orbital climate signal, as observed.

Differences in H-B and D-O, then, are likely related to oceanic feedbacks, as discussed next.

Synthesis

Mid-latitude continental ice sheets have grown and shrunk largely in response to changes in the seasonal distribution of solar heating linked to features of the Earth's orbit, as modulated through the dynamics of those ice sheets. Global cooling has been linked to ice growth during cool, short summers at high northern latitudes, with a much smaller role for solar-radiation anomalies elsewhere, suggesting important controls for synchronizing the hemispheres.

The presence of mid-latitude continents in the north (but not the south) is probably critical. Large land-ice fluctuations driving changes in ice albedo, sea level—hence possibly CO_2—and other factors can occur only in the north. Controls on CO_2 are especially problematic (Broecker 1995), but global ice volume (hence sea-level fall) and CO_2 show a strong inverse correlation, and many plausible mechanisms exist by which changes in sea level, temperature, windiness, and other factors could influence CO_2 (Broecker 1995).

Ice-albedo and CO_2 feedbacks cause changes in atmospheric and shallow oceanic circulation that further amplify the climate changes. Extratropical cooling increases the equator-to-pole temperature gradient and thus the wind strength. Stronger winds increase tropical upwelling and other mixing processes, cooling surface waters, reducing tropical water vapor, and thus causing additional cooling in and beyond the tropics. Cold northern conditions tend to weaken African and Asian monsoons, reducing tropical water vapor and also affecting cross-equatorial exchange. These processes have contributed to synchronizing the hemispheres.

The most recent deglaciation has been punctuated by millennial-scale warming and cooling events. Changes were large and rapid around the North Atlantic, and probably smaller and slower elsewhere. The changes may represent some combination of response to a free oscillation or oscillations in the climate system, and forced oscillations linked to changes in the mid-latitude ice sheets changing water and iceberg drainage from their margins. Most or all of the deglacial events are traceable to changes in the ice sheets and their meltwater routing, but this is not (yet) known to be true for some of the events during the growth of the mid-latitude ice sheets. The roughly consistent spacing of the events suggests a preferred timescale in any case, possibly linked to oceanic processes.

The abrupt climate changes are linked to reduction or elimination of North Atlantic deep water formation. Three suggested modes of operation (Sarnthein et al 1994, Stocker 1998) are modern, with vigorous high-latitude

formation of North Atlantic deep water through release of heat to the atmosphere that warms Greenland and Northern Europe; glacial, with vigorous formation of North Atlantic intermediate water and shallower North Atlantic deep water at lower latitude that does not provide much heat to Greenland and Northern Europe; and Heinrich, with greatly reduced sinking in the North Atlantic that leads to more rapid formation of Antarctic bottom waters and warming of some southern regions centered on the South Atlantic. The modern state applies to warm times, and cold times may reach the glacial or Heinrich modes. More data are needed, but the Heinrich mode appears to have caused, or been caused by, the larger, longer-lasting cold events of the North Atlantic and especially the Heinrich-event surges of the Laurentide ice sheet.

The modern-to-glacial switch greatly cools the high-latitude North Atlantic. Effects are transmitted through the atmosphere to the North Pacific (Behl and Kennett 1996, Mikolajewicz et al 1997), the monsoon belt of Africa and Asia (Street-Perrott & Perrott 1990), and other regions. Prominent methane changes occur for glacial-interglacial and D-O changes, related to high-latitude and monsoon-belt effects (Chappellaz et al 1993). Glacial-maximum and D-O cooling are both associated with the modern-to-glacial switch in ocean circulation. D-O events are too short to allow the large changes in CO_2 (Stauffer et al 1998), ice sheets and sea level that produce large global climate changes on the slower orbital timescale. The North Atlantic circulation spends most of its time during interglacials in the modern (hot) mode, and most of its time during glacials in the glacial mode. D-O oscillations represent jumps between these modes during transitional times.

The additional freshwater supply of H events forces jumps to the Heinrich mode, which have a smaller effect on the North Atlantic atmosphere than do D-O oscillations because the heat transport to the high-latitude North Atlantic cannot be reduced much more, but have a larger effect on the ocean circulation because they shut down NADW formation and reduce NAIW formation, creating a "demand" for deepwater formation elsewhere. These oceanic changes during Heinrich coolings cause a temperature seesaw in which most of the Earth follows the north Atlantic but with antiphase, probably slightly lagged behavior centered on the South Atlantic and likely involving other regions (Lund & Mix 1998). CO_2, which is primarily controlled by oceanic processes, changes during H events (Stauffer et al 1998).

The most direct tests of this synthesis would be provided by additional well-dated, high-resolution climate-change records, especially from the Antarctic continent, the Pacific sector of the southern ocean, tropical oceans and the North Pacific. Improved interpretation of paleoclimatic proxies, and improved modeling, would also be highly beneficial.

ACKNOWLEDGMENTS

We thank Michael Bender, Lloyd Keigwin, Jerry McManus, Alan Mix, and Thomas Stocker for helpful discussions, and Edouard Bard, Thomas Blunier, Gerard Bond, Ed Brook, Chris Charles, Haflidi Haflidason, Konrad Hughen, Lloyd Keigwin, Laurent Labeyrie, Scott Lehman, Alan Mix, Anne de Vernal, Todd Sowers, and Rainer Zahn for generously sharing data. NSF grants to Alley and Clark provided support for this paper.

Literature Cited

Alley RB, Anandakrishnan S, Cuffey KM. 1996. Subglacial sediment transport and ice stream behavior. *Antarct. J. US.* 31:81–82

Alley RB, Finkel RC, Nishiizumi K, Anandakrishnan S, Shuman CA, et al. 1995. Changes in continental and sea-salt atmospheric loadings in central Greenland during the most recent deglaciation. *J. Glaciol.* 41:503–14

Alley RB, MacAyeal DR. 1994. Ice-rafted debris associated with binge/purge oscillations of the Laurentide Ice Sheet. *Paleoceanography* 9:503–11

Alley RB, Mayewski PA, Sowers T, Stuiver M, Taylor KC, Clark PU. 1997. Holocene climatic instability: A prominent, widespread event 8200 years ago. *Geology* 25:483–86

Alley RB, Meese DA, Shuman CA, Gow AJ, Taylor KC, et al. 1993. Abrupt increase in snow accumulation at the end of the Younger Dryas event. *Nature* 362:527–29

Andreasen DJ, Ravelo AC. 1997. Tropical Pacific Ocean thermocline depth reconstructions for the last glacial maximum. *Paleoceanography* 12:395–413

Andrews JT, Erlenkeuser H, Tedesco K, Aksu AE, Jull AJT. 1994. Late Quaternary (Stage 2 and 3) meltwater and Heinrich events, northwest Labrador Sea. *Quat. Res.* 41:26–34

Andrews JT, Tedesco K. 1992. Detrital carbonate-rich sediments, northwestern Labrador Sea: implications for ice-sheet dynamics and iceberg rafting (Heinrich) events in the North Atlantic. *Geology* 20:1087–90

Bard E, Arnold M, Fairbanks RG, Hamelin B. 1993. ^{230}Th-^{234}U and ^{14}C ages obtained by mass spectrometry on corals. *Radiocarbon* 35:191–99

Bard E, Arnold M, Mangerud J, Paterne M, Labeyrie L, et al. 1994. The North Atlantic atmosphere-sea surface ^{14}C gradient during the Younger Dryas climatic event. *Earth Planet. Sci. Lett.* 126:275–87

Bard E, Arnold M, Maurice P, Duprat J, Moyes J, Duplessy JC. 1987. Retreat velocity of the North Atlantic polar front during the last deglaciation determined by ^{14}C accelerator mass spectrometry. *Nature* 328:791–94

Bard E, Hamelin B, Arnold M, Montaggioni L, Cabioch G, et al. 1996. Deglacial sea-level record from Tahiti corals and the timing of global meltwater discharge. *Nature* 382:241–44

Bard E, Rostek F, Sonzogni C. 1997. Interhemispheric synchrony of the last deglaciation inferred from alkenone palaeothermometry. *Nature* 385:707–10

Behl RJ, Kennett JP. 1996. Brief interstadial events in the Santa Barbara basin, NE Pacific, during the past 60 kyr. *Nature* 379:243–46

Bender ML. 1998. Interhemispheric phasing of millennial-duration climate events during the last 100 ka. *AGU Chapman Conf. Mechanisms of Millennial-Scale Global Climate Change. Abstracts with Program*, p. 10

Bender M, Sowers T, Dickson M-L, Orchardo J, Grootes P, et al. 1994. Climate correlations between Greenland and Antarctica during the past 100,000 years. *Science* 372:663–66

Benson LV, Burdett JW, Kashgarian M, Lund SP, Phillips FM, Rye RO. 1996. Climatic and hydrologic oscillations in the Owens Lake basin and adjacent Sierra Nevada, California. *Science* 274:746–49

Blunier T, Chappellaz J, Schwander J, Dällenbach A, Stauffer B, Stocker TF, Raynaud D, Jouzel J, Clausen HB, Hammer CU, Johnsen SJ. 1998. Asynchrony of Antarctic and Greenland climate change during the last glacial period. *Nature* 394:739–43

Benson LV, Lund SP, Burdett JW, Kashgarian

M, Rose TP, et al. 1998. Correlation of Late-Pleistocene lake-level oscillations in Mono Lake, California, with North Atlantic climate events. *Quat. Res.* 49:1–10

Beveridge NAS, Elderfield H, Shackleton NS. 1995. Deep thermohaline circulation in the low-latitude Atlantic during the last glacial. *Paleoceanography* 10:643–60

Birchfield GE, Broecker WS. 1990. A salt oscillator in the glacial Atlantic? 2. A "scale analysis" model. *Paleoceanography* 5:835–43

Blunier T, Schwander J, Stauffer B, Stocker T, Dallenbach A, et al. 1997. Timing of the Antarctic cold reversal and the atmospheric CO_2 increase with respect to the Younger Dryas event. *Geophys. Res. Lett.* 24:2683–86

Boden P, Fairbanks RG, Wright JD, Burckle LH. 1997. High-resolution stable isotope records from southwest Sweden: The drainage of the Baltic ice lake and Younger Dryas ice margin oscillations. *Paleoceanography* 12:39–49

Bond G, Broecker W, Johnsen S, McManus J, Labeyrie L, et al. 1993. Correlations between climate records from North Atlantic sediments and Greenland ice. *Nature* 365:143–47

Bond G, Heinrich H, Broecker W, Labeyrie L, McManus J, et al. 1992. Evidence for massive discharges of icebergs into the North Atlantic ocean during the last glacial period. *Nature* 360:245–49

Bond GC, Lotti R. 1995. Iceberg discharges into the North Atlantic on millennial time scales during the last deglaciation. *Science* 267:1005–10

Bond G, Showers W, Cheseby M, Lotti R, Almasi P, et al. 1997. A pervasive millennial-scale cycle in North Atlantic Holocene and glacial climates. *Science* 278:1257–66

Boyle E. 1995. Last-glacial-maximum North Atlantic deep water: on, off or somewhere in-between? *Philos. Trans. R. Soc. London Ser. B* 348:243–53

Boyle EA, Keigwin L. 1987. North Atlantic thermohaline circulation during the past 20,000 years linked to high-latitude surface temperature. *Nature* 330:35–40

Boyle EA, Keigwin LD. 1982. Deep circulation of the North Atlantic over the last 200,000 years: geochemical evidence. *Science* 218:784–87

Broecker WS. 1995. *The Glacial World According to Wally*. Palisades, NY: Lamont-Doherty Earth Obs. 318 pp.

Broecker WS. 1997. Mountain glaciers: recorders of atmospheric water vapor content? *Glob. Biogeochem. Cycles* 11:589–97

Broecker WS. 1998. Paleocean circulation during the last deglaciation: A bipolar seesaw? *Paleoceanography* 13:119–21

Broecker WS, Andree M, Wolfli W, Oeschger H, Bonani G, et al. 1988. The chronology of the last deglaciation: Implications to the cause of the Younger Dryas event. *Paleoceanography* 3:1–19

Broecker WS, Bond G, Klas M. 1990. A salt oscillator in the glacial Atlantic? 1. The concept. *Paleoceanography* 5:469–77

Broecker WS, Denton GH. 1989. The role of ocean-atmosphere reorganization in glacial cycles. *Geochim. Cosmochim. Acta* 53:2465–501

Broecker WS, Kennett JP, Flower BP, Teller JT, Trumbore S, et al. 1989. Routing of meltwater from the Laurentide ice sheet during the Younger Dryas cold episode. *Nature* 341:318–21

Brook EJ, Sowers T, Orchardo J. 1996. Rapid variations in atmospheric methane concentration during the past 110,000 years. *Science* 273:1087–1091

Bush ABG, Philander SGH. 1998. The role of ocean-atmosphere interactions in tropical cooling during the last glacial maximum. *Science* 279:1341–44

Chappell J, Omura A, Esat T, McCulloch M, Pandolfi J, et al. 1996. Reconciliation of late Quaternary sea levels derived from coral terraces at Huon Peninsula with deep sea oxygen isotope records. *Earth Planet. Sci. Lett.* 141:227–36

Chappellaz J, Blunier T, Raynaud D, Barnola JM, Schwander J, Stauffer B. 1993. Synchronous changes in atmospheric CH_4 and Greenland climate between 40 and 8 kyr b.p. *Nature* 366:443–45

Charles CD, Fairbanks RG. 1992. Evidence from Southern Ocean sediments for the effect of North Atlantic deep-water flux on climate. *Nature* 355:416–18

Charles CD, Lynch-Stieglitz J, Ninnemann US, Fairbanks RG. 1996. Climate connections between the hemispheres revealed by deep sea sediment core/ice core correlations. *Earth Planet. Sci. Lett.* 142:19–27

Clark PU. 1994. Unstable behavior of the Laurentide ice sheet over deforming sediment and its implications for climate change. *Quat. Res.* 41:19–25

Clark PU, Alley RB, Keigwin LD, Licciardi JM, Johnsen SJ, Wang HX. 1996. Origin of the first global meltwater pulse following the last glacial maximum. *Paleoceanography* 11:563–77

Clark PU, Bartlein PJ. 1995. Correlation of late Pleistocene glaciation in the western United States with North Atlantic Heinrich events. *Geology* 23:483–86

Cortijo E, Labeyrie L, Vidal L, Vautravers M, Chapman M, et al. 1997. Changes in sea surface hydrology associated with Heinrich event 4 in the North Atlantic Ocean between 40° and 60°N. *Earth Planet. Sci. Lett.* 146:29–45

Crowley TJ. 1992. North Atlantic deep water cools the southern hemisphere. *Paleoceanography* 7:489–97

Crowley TJ, Baum SK. 1997. Effect of vegetation on an ice-age climate model simulation. *J. Geophys. Res.* 102:16463–80

Curry WB, Lohmann GP. 1983. Reduced advection into Atlantic Ocean deep eastern basins during last glaciation maximum. *Nature* 306:577–80

Curry WB, Oppo DW. 1997. Synchronous, high-frequency oscillations in tropical sea surface temperatures and North Atlantic deep water production during the last glacial cycle. *Paleoceanography* 12:1–14

Denton GH, Hendy CH. 1994. Documentation of an advance of New Zealand's Franz Josef Glacier at the onset of Younger Dryas time. *Science* 264:1434–37

de Vernal A, Hillaire-Marcel C, Bilodeau G. 1996. Reduced meltwater outflow from the Laurentide ice margin during the Younger Dryas. *Nature* 381:774–77

Duplessy JC, Labeyrie L, Arnold M, Paterne M, Duprat J, van Weering DCE. 1992. Changes in surface salinity of the North Atlantic ocean during the last deglaciation. *Nature* 358:485–87

Edwards RL, Beck JW, Burr GS, Donahue DJ, Chappell J, et al. 1993. A large drop in atmospheric $^{14}C/^{12}C$ and reduced melting in the Younger Dryas, documented with ^{230}Th ages of corals. *Science* 260:962–68

Fanning AF, Weaver AJ. 1997. Temporal-geographical meltwater influences on the North Atlantic conveyor: Implications for the Younger Dryas. *Paleoceanography* 12:307–20

Fairbanks RG. 1989. A 17,000-year glacio-eustatic sea level record: influence of glacial melting rates on the Younger Dryas event and deep-ocean circulation. *Nature* 342:637–42

Fairbanks RG, Charles CD, Wright JD. 1992. Origin of global meltwater pulses. *Radiocarbon* (*After Four Decades*), p. 473–500

Finkel RC, Nishiizumi K. 1997. Beryllium 10 concentrations in the Greenland Ice Sheet Project 2 ice core from 3-40 ka. *J. Geophys. Res.* 102:26699–706

Ganopolski A, Rahmstorf S, Petouknov V, Claussen M. 1998. Simulation of modern and glacial climates with a coupled global model of intermediate complexity. *Nature* 319:351–56

Genthon C, Barnola JM, Raynaud D, Lorius C, Jouzel J, et al. 1987. Vostok ice core: Climatic response to CO_2 and orbital forcing changes over the last climatic cycle. *Nature* 329:414–18

Grimm EC, Jacobson GL Jr, Watts WA, Hansen BCS, Maasch KA. 1993. A 50,000-year record of climate oscillations from Florida and its temporal correlation with the Heinrich events. *Science* 261:198–200

Grootes PM. 1993. Interpreting continental oxygen isotope records. In *Climate Change in Continental Isotopic Records. Am. Geophys. Union Geophys. Monogr.* 78:37–46

Grootes PM, Stuiver M. 1997. Oxygen 18/16 variability in Greenland snow and ice with 10^{-3}- to 10^{5}-year time resolution. *J. Geophys. Res.* 102:26455–70

Grootes PM, Stuiver M, White JWC, Johnsen SJ, Jouzel J. 1993. Comparison of oxygen isotope records from the GISP2 and GRIP Greenland ice cores. *Nature* 366:552–54

Grousset FE, Labeyrie L, Sinko JA, Cremer M, Bond G, et al. 1993. Patterns of ice-rafted detritus in the glacial North Atlantic (40-55°N). *Paleoceanography* 8:175–92

Gwiazda RH, Hemming SR, Broecker WS. 1996a. Provenance of icebergs during Heinrich event 3 and the contrast to their sources during other Heinrich episodes. *Paleoceanography* 11:371–78

Gwiazda RH, Hemming SR, Broecker WS, Onsttot T, Mueller C. 1996b. Evidence from $^{40}Ar/^{39}Ar$ ages for a Churchill province source of ice-rafted amphiboles in Heinrich layer 2. *J. Glaciol.* 42:440–46

Haflidason H, Sejrup HP, Kristensen DK, Johnsen S. 1995. Coupled response of the late glacial climatic shifts of northwest Europe reflected in Greenland ice cores: Evidence from the northern North Sea. *Geology* 23:1059–62

Hays HD, Imbrie J, Shackleton NJ. 1976. Variations in the earth's orbit: pacemaker of the ice ages. *Science* 194:1121–32

Heinrich H. 1988. Origin and consequences of cyclic ice rafting in the northeast Atlantic Ocean during the past 130,000 years. *Quat. Res.* 29:143–52

Hesse R, Khodabakhsh S. 1998. Depositional facies of late Pleistocene Heinrich events in the Labrador Sea. *Geology* 26:103–6

Hostetler SW, Clark PU, Bartlein PJ, Mix AC, Pisias NG. 1999. Atmospheric transmission of North Atlantic Heinrich events. *J. Geophys. Res.* (in press)

Hughen KA, Overpeck JT, Peterson LC, Trumbore S. 1996. Rapid climate changes in the tropical Atlantic region during the last deglaciation. *Nature* 380:51–54

Hulbe CL. 1997. An ice shelf mechanism for

Heinrich layer production. *Paleoceanography* 12:711–17

Imbrie J, Berger A, Boyle EA, Clemens SC, Duffy A, et al. 1993. On the structure and origin of major glaciation cycles: 2. The 100,000-year cycle. *Paleoceanography* 8: 699–735

Imbrie J, Boyle EA, Clemens SC, Duffy A, Howard WR, et al. 1992. On the structure and origin of major glaciation cycles 1. Linear responses to Milankovitch forcing. *Paleoceanography* 7:701–38

Imbrie J, Hays JD, Martinson DG, McIntyre A, Mix AC, et al. 1984. The orbital theory of Pleistocene climate: Support from a revised chronology of the marine $\delta^{18}O$ record. In *Milankovitch and Climate, Part I*, ed. A Berger J Imbrie, J Hays, G Kukla, B Saltzman, p. 269–305. Norwell, MA: D Riedel. 895 pp.

Jansen E, Veum T. 1990. Evidence for two-step deglaciation and its impact on North Atlantic deep-water circulation. *Nature* 343:612–16

Jones GA, Keigwin LD. 1988. Evidence from Fram Strait (78°N) for early deglaciation. *Nature* 336:57–59

Jouzel J, Lorius C, Petit JR, Genthon C, Barkov NI, et al. 1987. Vostok ice core: A continuous isotope temperature record over the last climatic cycle (160,000 years). *Nature* 329:403–8

Jouzel J, Vaikmae R, Petit JR, Martin M, Duclos Y, et al. 1995. The two-step shape and timing of the last deglaciation in Antarctica. *Clim. Dyn.* 11:151–61

Keigwin LD, Jones GA. 1995. The marine record of deglaciation from the continental margin off Nova Scotia. *Paleoceanography* 10:973–85

Keigwin LD, Jones GA, Lehman SJ, Boyle E. 1991. Deglacial meltwater discharge, North Atlantic deep circulation, and abrupt climate change. *J. Geophys. Res.* 96:16811–26

Keigwin LD, Lehman SJ. 1994. Deep circulation change linked to Heinrich event 1 and Younger Dryas in a middepth North Atlantic core. *Paleoceanography* 9:185–94

Kitagawa H, van der Plicht J. 1998. Atmospheric radiocarbon calibrations to 45,000 yr B.P.: Late glacial fluctuations of cosmogenic isotope production. *Science* 279:1187–90

Koç N, Jansen E. 1994. Response of the high-latitude northern hemisphere to orbital climate forcing: Evidence from the Nordic seas. *Geology* 22:523–26

Labeyrie L, Labracherie M, Gorfti N, Pichon JJ, Vautravers M, et al. 1996. Hydrographic changes of the Southern ocean (southeast Indian sector) over the last 230 kyr. *Paleoceanography* 11:57–76

Labeyrie LD, Duplessy JC, Duprat J, Juillet-Leclerc A, Moyes J, et al. 1992. Changes in the vertical structure of the North Atlantic ocean between glacial and modern times. *Quat. Sci. Rev.* 11:401–13

Labeyrie L, Vidal L, Cortijo E, Paterne M, Arnold M, et al. 1995. Surface and deep hydrology of the Northern Atlantic ocean during the past 150,000 years. *Philos. Trans. R. Soc. London Ser. B* 348:255–64

Labracherie M, Labeyrie LD, Duprat J, Bard E, Arnold M, et al. 1989. The last deglaciation in the southern ocean. *Paleoceanography* 4:629–38

Lal D, Jull AJT, Burr GS, Donahue DJ. 1997. Measurements of in situ ^{14}C concentrations in Greenland Ice Sheet Project 2 ice covering a 17-kyr time span: Implications to ice flow dynamics. *J. Geophys. Res.* 102:26505–10

Lehman SJ, Jones GA, Keigwin LD, Andersen ES, Butenko G, Ostmo SR. 1991. Initiation of Fennoscandian ice-sheet retreat during the last deglaciation. *Nature* 349:513–16

Lehman SJ, Keigwin LD. 1992a. Deep circulation revisited. *Nature* 358:197–98

Lehman SJ, Keigwin LD. 1992b. Sudden changes in the North Atlantic circulation during the last deglaciation. *Nature* 356:757–62

Lehman SJ, Wright DG, Stocker TF. 1993. Transport of freshwater into the deep ocean by the conveyor. *NATO ASI Ser. I* 12:187–209

Little MG, Schneider RR, Kroon D, Price B, Summerhayes CP, Segl M. 1997. Trade wind forcing of upwelling seasonality, and Heinrich events as a response to sub-Milankovitch climate variability. *Paleoceanography* 12:568–76

Lorius C, Jouzel J, Raynaud D, Hansen J, Le Treut H. 1990. The ice-core record: climate sensitivity and future greenhouse warming. *Nature* 347:139–45

Lowell TV, Heusser CJ, Andersen BG, Moreno PI, Hauser A, et al. 1995. Interhemispheric correlation of Late Pleistocene glacial events. *Science* 269:1541–49

Lund DC, Mix AC. 1998. Millennial-scale deep water oscillations: reflections of the North Atlantic in the deep Pacific from 10 to 60 ka. *Paleoceanography* 13:1–19

Lyle M. 1988. Climatically forced organic carbon burial in equatorial Atlantic and Pacific Oceans. *Nature* 335:529–32

MacAyeal DR. 1993. A low-order model of growth/purge oscillations of the Laurentide Ice Sheet. *Paleoceanography* 8:767–73

Maier-Raimer E, Mikolajewicz U. 1989. Experiments with an OGCM on the cause of the Younger Dryas. In *Oceanography, 1988*, ed. A Ayala-Castanares, W Wooster, A Yanez-Arancibia, p. 87–100. Mexico City: Univ. Nac. Auton. Mex. Press

Manabe S, Broccoli AJ. 1985. The influence of continental ice sheets on the climate of an ice age. *J. Geophys. Res.* 90:2167–90

Manabe S, Stouffer RJ. 1997. Coupled ocean-atmosphere model response to freshwater input: Comparison to Younger Dryas event. *Paleoceanography* 12:321–36

Marcantonio F, Anderson RF, Stute M, Kumar N, Schlosser P, Mix A. 1996. Extraterrestrial ^{3}He as a tracer of marine sediment transport and accumulation. *Nature* 383:705–7

Marshall SJ, Clarke GKC. 1997. A continuum mixture model of ice stream thermomechanics in the Laurentide Ice Sheet. 2. Application to the Hudson Strait ice stream. *J. Geophys. Res.* 102:20615–37

Maslin MA, Shackleton NJ, Pflaumann U. 1995. Surface water temperature, salinity, and density changes in the northeast Atlantic during the last 45,000 years: Heinrich events, deep water formation, and climatic rebounds. *Paleoceanography* 10:527–44

Mayewski PA, Meeker LD, Twickler MS, Whitlow S, Yang Q, et al. 1997. Major features and forcing of high-latitude northern hemisphere atmospheric circulation using a 110,000-year-long glaciochemical series. *J. Geophys. Res.* 102:26345–66

Mayewski PA, Twickler MS, Whitlow SI, Meeker LD, Yang Q, et al. 1996. Climate change during the last deglaciation in Antarctica. *Science* 272:1636–38

McCabe AM, Clark PU. 1998. Ice-sheet variability around the North Atlantic Ocean during the last deglaciation. *Nature* 392:373–77

McIntyre A, Molfino, B. 1996. Forcing of Atlantic equatorial and subpolar millennial cycles by precession. *Science* 274:1867–70

McManus JF, Anderson RF, Broecker WS, Fleisher MQ, Higgins SM. 1998. Radiometrically determined sedimentary fluxes in the sub-polar North Atlantic during the last 140,000 years. *Earth Planet. Sci. Lett.* 155:29–43

Mikolajewicz U, Crowley TJ, Schiller A, Voss R. 1997. Modeling teleconnections between the North Atlantic and North Pacific during the Younger Dryas. *Nature* 387:384–7

Mix AC, Ruddiman WF, McIntyre A. 1986. Late Quaternary paleoceanography of the tropical Atlantic, 1: Spatial variability of annual mean sea-surface temperatures, 0-20,000 years bp. *Paleoceanography* 1:43–66

Mooers HD, Lehr JD. 1997. Terrestrial record of Laurentide Ice Sheet reorganization during Heinrich events. *Geology* 25:987–90

Mulder T, Moran K. 1995. Relationship among submarine instabilities, sea level variations, and the presence of an ice sheet on the continental shelf, An example from the Verrill Canyon Area, Scotian Shelf. *Paleoceanography* 10:137–54

Muller RA, MacDonald GJ. 1997. Glacial cycles and astronomical forcing. *Science* 277: 215–18

Oerlemans J. 1993. Evaluating the role of climate cooling in iceberg production and the Heinrich events. *Nature* 364:783–86

Oppo DW, Lehman SJ. 1993. Mid-depth circulation of the subpolar North Atlantic during the last glacial maximum. *Science* 259:1148–52

Oppo DW, Lehman SJ. 1995. Suborbital timescale variability of North Atlantic Deep Water formation during the last 200,000 years. *Paleoceanography* 12:191–205

Patrick A, Thunell RC. 1997. Tropical Pacific sea surface temperatures and upper water column thermal structure during the last glacial maximum. *Paleoceanography* 12:649–57

Peteet DM, ed. 1993. Global Younger Dryas, a special issue of *Quat. Sci. Rev.* 12:277–355 (Suppl.)

Phillips FM, Zreda MG, Benson LV, Plummer MA, Elmore D, Sharma P. 1996. Chronology for fluctuations in Late Pleistocene Sierra Nevada glaciers and lakes. *Science* 274:749–51

Pichon JJ, Labeyrie LD, Bareille G, Labracherie M, Duprat J, Jouzel J. 1992. Surface water temperature changes in the high latitudes of the southern hemisphere over the last glacial-interglacial cycle. *Paleoceanography* 7:289–318

Pisias NG, Mix AC. 1997. Spatial and temporal oceanographic variability of the eastern equatorial Pacific during the late Pleistocene: evidence from radiolaria microfossils. *Paleoceanography* 12:381–93

Pollard D, Thompson SL. 1997. Climate and ice-sheet mass balance at the last glacial maximum from the GENESIS Version 2 global climate model. *Quat. Sci. Rev.* 16:841–64

Porter SC, An Z. 1995. Correlation between climate events in the North Atlantic and China during the last glaciation. *Nature* 375:305–8

Rahmstorf S. 1995. Bifurcations of the Atlantic thermohaline circulation in response to changes in the hydrological cycle. *Nature* 378:145–49

Rasmussen TL, Thomsen E, van Weering TCE, Labeyrie L. 1996. Rapid changes in surface and deep water conditions at the Faeroe Margin during the last 58,000 years. *Paleoceanography* 11:757–72

Raymo ME. 1997. The timing of major climate terminations. *Paleoceanography* 12:577–85

Rea DK. 1994. The paleoclimatic record pro-

vided by eolian deposition in the deep sea: the geologic history of wind. *Rev. Geophys.* 32:159–95

Revel M, Sinko JA, Grousset FE, Biscaye PE. 1996. Sr and Nd isotopes as tracers of North Atlantic lithic particles: paleoclimatic implications. *Paleoceanography* 11:95–113

Sakai K, Peltier WR. 1995. A simple model of the Atlantic thermohaline circulation: internal and forced variability with paleoclimatological implications. *J. Geophys. Res.* 100:13,455–79

Salamatin AN, Lipenkov VY, Barkov NI, Jouzel J, Petit JR, Raynaud D. 1998. Ice core age dating and paleothermometer calibration based on isotope and temperature profiles from deep boreholes at Vostok Station (East Antarctica). *J. Geophys. Res.* 103:8963–77

Sarnthein M, Jansen E, Weinelt M, Arnold M, Duplessy JC, et al. 1995. Variations in Atlantic surface ocean paleoceanography, 50°-80°N: Time-slice records of the last 30,000 years. *Paleoceanography* 10:1063–94

Sarnthein M, Winn K, Jung SJA, Duplessy JC, Labeyrie L, et al. 1994. Changes in east Atlantic deepwater circulation over the last 30,000 years: Eight time slice reconstructions. *Paleoceanography* 9:209–67

Schiller A, Mikolajewicz U, Voss R. 1997. The stability of the North Atlantic thermohaline circulation in a coupled ocean-atmosphere general circulation model. *Clim. Dyn.* 13:325–47

Schulz H, von Rad U, Erlenkeuser H. 1998. Correlation between Arabian Sea and Greenland climate oscillations of the past 110,000 years. *Nature* 393:54–57

Severinghaus JP, Sowers T, Brook EJ, Alley RB, Bender ML. 1998. Timing of abrupt climate change at the end of the Younger Dryas interval from thermally fractionated gases in polar ice. *Nature* 391:141–46

Sirocko F, Garbe-Schönberg D, McIntyre A, Molfino B. 1996. Teleconnections between the subtropical monsoons and high-latitude climates during the last deglaciation. *Science* 272:526–29

Sowers T, Bender M. 1995. Climate records covering the last deglaciation. *Science* 269: 210–14

Stauffer B, Blunier T, Dällenback A, Indermühle A, Schwander J et al. 1998. Atmospheric CO_2 concentration and millennial-scale climate change during the last glacial period. *Nature* 392:59–62

Steig EJ, Brook EJ, White JWC, Sucher CM, Bender ML, Lehman SJ, Morse DL, Waddington ED, Clow GD, 1998. Synchronous climate changes in Antarctica and the North Atlantic. *Science* 282:92–95

Stocker TF. 1998. Is there a unique mechanism for abrupt changes in the climate system? *AGU Chapman Conf. Mechanisms of Millennial-Scale Global Climate Change. Abstracts with Program*, p. 30

Stocker TF, Wright DG. 1996. Rapid changes in ocean circulation and atmospheric radiocarbon. *Paleoceanography* 11:773–95

Stocker TF, Wright DG, Broecker WS. 1992. The Influence of high-latitude surface forcing on the global thermohaline circulation. *Paleoceanography* 7:529–41

Stoner JS, Channell JET, Hillaire-Marcel C. 1996. The magnetic signature of rapidly deposited detrital layers from the deep Labrador Sea: relationship to North Atlantic Heinrich layers. *Paleoceanography* 11:309–26

Street-Perrott FA, Perrott RA. 1990. Abrupt climate fluctuations in the tropics: the influence of Atlantic Ocean circulation. *Nature* 358:607–12

Tarasov L, Peltier WR. 1997. A high-resolution model of the 100 ka ice-age cycle. *Ann. Glaciol.* 25:58–65

Taylor KC, Mayewski PA, Alley RB, Brook EJ, Gow AJ, et al. 1997. The Holocene/Younger Dryas transition recorded at Summit, Greenland. *Science* 278:825–7

Teller JT. 1990. Meltwater and precipitation runoff to the North Atlantic, Arctic, and Gulf of Mexico from the Laurentide ice sheet and adjacent regions during the Younger Dryas. *Paleoceanography* 5:897–905

Teller JT, Licciardi J, Clark PU. 1998. North American meltwater routing to the North Atlantic during the last deglaciation. AGU Chapman Conference, *Mechanisms of Millennial-Scale Global Climate Change. Abstracts with Program.* p. 26

Tziperman E. 1997. Inherently unstable climate behavior due to weak thermohaline ocean circulation. *Nature* 386:592–95

Veum T, Jansen E, Arnold M, Beyer I, Duplessy JC. 1992. Water mass exchange between the North Atlantic and the Norwegian Sea during the past 28,000 years. *Nature* 356:783–5

Vidal L, Labeyrie L, Cortijo E, Arnold M, Duplessy JC, et al. 1997. Evidence for changes in the North Atlantic Deep Water linked to meltwater surges during the Heinrich events. *Earth Planet. Sci. Lett.* 146:13–27

Weertman J. 1974. Stability of the junction of an ice sheet and ice shelf. *J. Glaciol.* 5:145–58

Weinelt M, Sarnthein M, Pflaumann U, Schulz H, Jung S, Erlenkeuser H. 1996. Ice-free Nordic Seas during the last glacial maximum? Potential sites of deepwater formation. *Paleoclimates* 1:283–309

Winograd IJ, Coplen TB, Landwehr JM, Riggs AC, Ludwig KR, et al. 1992. Continuous 500,000-year climate record from vein calcite

in Devils Hole, Nevada. *Science* 258:255–60

Yiou P, Genthon C, Ghil M, Jouzel J, Le Treut H, et al. 1991. High-frequency paleovariability in climate and CO_2 levels from Vostok ice core records. *J. Geophys. Res.* 96:20365–78

Yu EF, Francois R, Bacon MP. 1996. Similar rates of modern and last-glacial ocean thermohaline circulation inferred from radiochemical data. *Nature* 379:689–94

Zahn R, Schonfeld J, Kudrass HR, Park MH, Erlenkeuser H, Grootes P. 1997. Thermohaline instability in the North Atlantic during meltwater events: Stable isotope and ice-rafted detritus records from core SO75-26KL, Portugese margin. *Paleoceanography* 12:696–710

Annual Review of Earth and Planetary Science
Volume 27, 1999

CONTENTS